



Mishra, A., Ayasolla, K., Kumar, V., Lan, X., Vashistha, H., Aslam, R., ...
Singhal, P. C. (2018). Modulation of APOL1-miR193a Axis Prevents
Podocyte Dedifferentiation in High Glucose Milieu. *AJP - Renal Physiology*,
314(5), 832-843. <https://doi.org/10.1152/ajprenal.00541.2017>

Peer reviewed version

License (if available):
Other

Link to published version (if available):
[10.1152/ajprenal.00541.2017](https://doi.org/10.1152/ajprenal.00541.2017)

[Link to publication record in Explore Bristol Research](#)
PDF-document

This is the accepted author manuscript (AAM). The final published version (version of record) is available online via the American Physiological Society at <https://doi.org/10.1152/ajprenal.00541.2017> . Please refer to any applicable terms of use of the publisher.

University of Bristol - Explore Bristol Research

General rights

This document is made available in accordance with publisher policies. Please cite only the published version using the reference above. Full terms of use are available:
<http://www.bristol.ac.uk/pure/about/ebr-terms>

1 **Modulation of APOL1-miR193a Axis Prevents Podocyte**
2 **Dedifferentiation in High Glucose Milieu**

3
4
5
6
7
8
9 Abheepsa Mishra¹, Kamesh Ayasolla¹, Vinod Kumar¹, Xiqian LAN¹. Himanshu Vashistha²,
10 Rukhsana Aslam¹, Ali Hussain¹, Sheetal Chowdhary¹, Shadafarin Marashi Shoshtari¹,
11 Nitpriya Paliwal¹, Waldemar Popik³, Moin A. Saleem⁴, Ashwani Malhotra¹, Leonard G
12 Meggs², Karl Skorecki⁵, and Pravin C. Singhal¹

13
14
15 ¹Immunology and Inflammation center, Feinstein Institute for Medical Research and Zucker
16 School of Medicine at Hofstra-Northwell, New York, USA, ²Ochsner Clinic, New Orleans,
17 USA, ³Meharry Medical College, Nashville, TN, USA, ⁴Academic Renal Unit, University,
18 Bristol, Bristol, UK, ⁵Technion – Israel Institute of Technology, and Rambam Health Care
19 Campus, Haifa, Israel.

20
21
22
23
24 Address for Correspondence
25 Pravin C. Singhal, MD
26 Nephrology Division
27 100 Community Drive
28 Great Neck, NY 11021
29 E-mail psinghal@northwell.edu
30 Tel 516-465-3010
31 Fax 516-465-3011

32 Running head: Podocyte dedifferentiation and high glucose
33

34 **Abstract**

35 The loss of podocyte (PD) molecular phenotype is an important feature of diabetic
36 podocytopathy. We hypothesized that high glucose (HG) induces dedifferentiation in
37 differentiated podocytes (DPD) through alterations in APOL1-microRNA (miR) 193a axis.
38 HG-induced DPDs dedifferentiation manifested in the form of down regulation of WT1 and
39 upregulation of PAX2 expression. WT1- silenced DPDs displayed enhanced expression of
40 PAX2. Immunoprecipitation (IP) of DPD cellular lysates with anti-WT1 antibody revealed
41 formation of WT1 repressor complexes containing Polycomb group proteins (PcG), EZH2,
42 Menin, and DNA methyl transferase (DNMT1), whereas, silencing of either WT1 or DNMT1
43 disrupted this complex with enhanced expression of PAX2. HG-induced DPDs
44 dedifferentiation was associated with a higher expression of miR193a, whereas, inhibition
45 of miR193a prevented DPDs dedifferentiation in HG milieu. HG down regulated DPDs
46 expression of APOL1. MiR193a-overexpressing DPDs displayed down regulation of APOL1
47 and enhanced expression of dedifferentiating markers; conversely, silencing of miR193a
48 enhanced the expression of APOL1 and also preserved DPDs phenotype. Moreover, stably
49 APOL1G0-overexpressing DPDs displayed the enhanced expression of WT1 but
50 attenuated expression of miR193a; nonetheless, silencing of APOL1 reversed these
51 effects. Since silencing of APOL1 enhanced miR193a expression as well as
52 dedifferentiation in DPDs, it appears that down regulation of APOL1 contributed to
53 dedifferentiation of DPDs through enhanced miR193a expression in HG milieu. Vitamin D
54 receptor agonist (VDA) down regulated miR193a, upregulated APOL1 expression, and
55 prevented dedifferentiation of DPDs in HG milieu. These findings suggest that modulation
56 of the APOL1-miR193a axis carries a potential to preserve DPDs molecular phenotype in
57 HG milieu.

58 Podocytes play a key role in the maintenance of slit diaphragm, a component of the
59 glomerular filtration barrier (5, 32, 33). Slit diaphragms are composed of several proteins
60 expressed by podocytes and prevent leakage of plasma proteins (32, 33). An optimal
61 expression of the slit diaphragm proteins is considered to be an integral part of podocyte
62 health. Since both parietal epithelial cells (PECs) and podocytes (PDS) are derived from
63 the same mesenchymal cells during embryogenesis (26, 37), injured adult podocytes go
64 into dedifferentiation mode- reverting to the expression of PEC markers such as paired
65 homeo box (PAX)-2 (31, 35, 39). High glucose milieu has been demonstrated to induce
66 dedifferentiation of PDs as a manifestation of PD injury (2, 16, 18, 37). However, the
67 mechanisms involved are not clear.

68 PAX2 is a transcription factor which plays an important role in the development of
69 kidneys (9-11, 38). In adult kidney, its expression is restricted to glomerular parietal and
70 tubular epithelial cells (10). However, ectopic PAX2 expression in podocytes is a common
71 finding in several pathological states including juvenile nephronophthisis (28), focal
72 segmental glomerulosclerosis (30, 31), collapsing glomerulopathy (7), and diabetic
73 glomerulosclerosis (2, 25). Since PAX2 is involved in cellular proliferation (43), this disease
74 state expression may be an attempt by podocytes to regenerate in adverse milieus. In a
75 mouse model of podocyte injury, evaluation of PDs dedifferentiation in podocyte reporter
76 mice demonstrated that PDs expressing PECs markers (PAX2/PAX8) far exceed PECs
77 expressing PD markers (33).

78 MicroRNAs (miRs) are small, non-coding RNAs that negatively regulate gene
79 expression at the post-transcription level (1). By an imperfect sequence complementation,
80 miRNAs recognize and bind to the 3'-untranslated regions (3'-UTR) of target mRNAs,

81 thereby inhibiting mRNA function through degradation, repression of translation, or both.
82 Recently, miR193a has been demonstrated to induce down regulation of WT1 in podocytes
83 (25). miR193a is tumor suppressor gene inducing apoptosis in podocytes through
84 generation of oxidative stress. However, the role of miR193a in high glucose-induced PD
85 dedifferentiation has not been reported (29). Since WT1 inversely regulate PAX2
86 expression (8, 34), we hypothesize that high glucose would induce PAX2 expression
87 through down regulation of WT1 and enhanced PD expression of miR193a.

88 APOL1 is a minor component of High-Density Lipoprotein (HDL) complex and is
89 expressed in kidney cells including podocytes, tubular cells, and other cell types (42). It is
90 predominantly secreted by liver cells and circulates in the plasma (42). The G1 variant is a
91 missense mutant haplotype (S342G:I384M), encoding two non-synonymous amino acids;
92 while the G2 variant is a 6 bp in-frame deletion resulting in loss of two amino acids (N388
93 and Y389) at the C-terminal helix of APOL1. Approximately 34% of African Americans
94 (AAs) carry one of the two risk variants and 13% have some combination of both coding
95 variants (41). Overt expression of APOL1G1 and G2 has been associated with podocyte
96 injury both *in vitro* and *in vivo* studies (3, 15, 23, 24). The trypanolytic activity of circulating
97 APOL1 (wild-type or G0) has been long appreciated and well characterized, though the
98 detailed molecular mechanism is not fully resolved (12). The function of APOL1G0 in
99 podocytes is not clearly understood. We hypothesize that high glucose induces PDs
100 dedifferentiation through down regulation of APOL1 and upregulation of microRNA (miR)
101 193a. We further hypothesize that modulation of APOL1-miR193a axis can be used as a
102 tool to preserve PDs differentiation in high glucose milieu.

103

104 **Material and Methods**

105 **Human podocytes**

106 Human podocytes (PDs) were conditionally immortalized by introducing
107 temperature-sensitive SV40-T antigen by transfection (36). These cells proliferate at the
108 permissive temperature (33°C) and enter growth arrest after transfer to the non-permissive
109 temperature (37°C). The growth medium contains RPMI 1640 supplemented with 10% fetal
110 bovine serum (FBS), 1x Pen-Strep, 1 mM L-glutamine and 1x ITS (Invitrogen).
111 Undifferentiated (UND) PDs were seeded on collagen coated plates and differentiated
112 through pre-incubation in normal RPMI (containing 11 mM glucose) for 10 days at 37°C
113 (differentiated podocytes, DPDs). Prior to experimental protocols, DPDs were washed three
114 times with glucose- and serum-free media. In experimental protocols, DPDs were
115 incubated in media (glucose- and ITS-free RPMI) containing either normal glucose (5 mM)
116 or high glucose (30 mM) for 48 h. DNA sequencing of these podocytes revealed *APOL1G0*
117 genotype.

118 **Generation of a stable cell lines expressing *APOL1G0* and Vector**

119 A stable cell line expressing *APOL1G0* was generated by retroviral infection as
120 described previously (27). Briefly, the open reading frame of *APOL1G0* was cloned into the
121 retroviral vector pBABE carrying resistance to puromycin. To generate retroviral particles,
122 the viral packaging cell line HEK-GP was co-transfected with the pBABE construct of
123 interest and the VSV gene. Undifferentiated podocytes (UNDPDs) were infected twice
124 within 24 h with the viral-containing supernatant of HEK-GP cells. Selection with puromycin
125 (1 µg/mL) was continued for a week, and expression of the sequence of the *APOL1G0* was

126 verified. Empty vector pBABE-eGFP was also transduced into UNDPDs to generate the
127 control cell line.

128 **Transfection of miR193a inhibitor and miR193a expression plasmid**

129 miR193a inhibitor (25 nM; Cat #4464084;Thermofisher, USA), miR193a expression
130 plasmid (25 nM; Cat #SC400232; Origene), and empty vector (25 nM; pCMV-MIR;
131 Origene) were transfected in the cells using Lipofectamine 3000 Transfection Reagent
132 (Thermo Fisher Scientific, USA) according to the manufacturer's protocol. All miRNA
133 products were dissolved in nuclease-free water. Briefly, DPDs were transfected at 70 - 80%
134 confluence in 6 well plates. The Lipofectamine transfection reagent (7.5 µl) and plasmid
135 DNA were diluted in opti-MEM media (125 µl and 250 µl) (Applied Biosystems, Thermo
136 Fisher Scientific, USA) followed by addition of P3000 enhancer reagent (10 µl) to diluted
137 DNA. Diluted DNA (125 µl) was added to diluted Lipofectamine 3000 transfection reagent
138 (125 µl) in the ratio of 1:1 (v/v) and incubated for 10 min at room temperature (25°C). After
139 incubation, DNA-lipid complex was added to the cells and kept at 37°C in opti-MEM media
140 for 48 hrs. Control and transfected cells were harvested for protein and RNA analyses.

141 **Vitamin D Receptor agonist (VDA) treatment**

142 Vitamin D Receptor agonist (VDA; EB1089, 10 nM; Tocris, MN, USA) was used to
143 modulate the expression of miR193a. VDA (2.2 mM) was initially dissolved in 10% DMSO
144 (100 µl) and diluted further with sterile PBS buffer (pH 7.2) to achieve final working
145 concentrations of 10 µM and 1µM. The final concentration of DMSO was 0.1 % in the
146 vehicle in all the experiments. DPDs in the experimental conditions were treated with VDA
147 for 48 h and harvested for protein and RNA for further analyses.

148 **Silencing of APOL1, WT1, and DNMT1**

149 DPDs were transfected with scrambled siRNA (control) or APOL1 siRNA (20 nM;
150 Santa Cruz), WT1 siRNA (25 nM; Santa Cruz), DNMT1 (25 nM; Santa Cruz) with
151 Lipofectamine RNAiMAX transfection reagent according to the manufacturer's protocol
152 (Thermo Fisher). Briefly, DPDs were transfected at 60-80% confluence in 6 well plates.
153 Lipofectamine reagent (9 μ l) and siRNAs (10 μ M, 2-3 μ l) were diluted in opti-MEM media
154 (150 μ l) (Thermo Fisher). Then, diluted siRNA (150 μ l) was added to diluted Lipofectamine
155 reagent (150 μ l) in 1:1 ratio (v/v) and incubated for 5 min at room temperature (25°C). After
156 incubation, the siRNA lipid-complex was added to cells and kept at 37°C in opti-MEM
157 media for 48 hrs. The cells were harvested for protein and RNA analyses. Control and
158 transfected cells were used under control and experimental conditions.

159 **RNA isolation and qPCR studies**

160 Total RNA was isolated from control and experimental DPDs with TRIzol reagent
161 (Invitrogen, USA). A 20 μ l reaction mix was prepared containing iTaq Universal SYBR
162 Green reaction mix (2x) (10 μ l), iscript reverse transcriptase (0.25 μ l), forward and reverse
163 primers (2 μ l), RNA (4 μ l), and nuclease free water (3.75 μ l). Real-Time PCR was
164 performed using one-step iTaqTM Universal SYBR Green kit (BIO-RAD, USA) according to
165 the manufacturer's instructions using specific primers obtained from Thermo Fisher
166 Scientific, USA. *GAPDH* fw 5' CCC ATC ACC ATC TTC CAG GAG '3; rev 5' GTT GTC
167 ATG GAT GAC CTT GGC '3, *WT1* fw 5' CGAGAGCGATAACCCACACAACG '3; rev 5'
168 GTCTCAGATGCCGACCGTACAA '3, *PAX2*fw 5' GGC TGT GTC AGC AAA ATC CTG '3;
169 rev 5' TCC GGA TGA TTC TGT TGA TGG '3, *APOL1* fw 5' ATC TCA GCT GAA AGC GGT
170 GAAC '3; rev 5' TGA CTT TGC CCC CTC ATG TAAG '3. The qPCR conditions were as

171 follows: 50°C for 10 min 95°C for 1 min, followed by 40 cycles of 95°C for 15 s, 60°C for 1
172 min. Quantitative PCR was performed using an ABI Prism 7900HT sequence detection
173 system and relative quantification of gene expression was calculated using the $\Delta\Delta CT$
174 method. Data were expressed as relative mRNA expression in reference to the control,
175 normalized to the quantity of RNA input by performing measurements on an endogenous
176 reference gene (GAPDH).

177 **MicroRNA assay**

178 For miRNA quantification, the total RNA was isolated from control and experimental DPDs
179 with miRVana miRNA isolation kit and 1 μg of RNA was reverse transcribed using miR193a
180 and U6snRNA specific RT primers to generate first strand cDNA from mRNA using
181 TaqMan microRNA Reverse Transcription kit (Thermo Fisher Scientific, USA) according to
182 manufacturer's instructions. For cDNA, a 15 μl PCR reaction was prepared containing 100
183 mM dNTP mix (0.15 μl), multiscrite RT enzyme 50 U/ μl (1 μl), 10X RT buffer (1.5 μl),
184 RNase inhibitor 20 U/ μl (0.19 μl), nuclease free water (4.16 μl), RNA (5 μl), and primers (3
185 μl). The PCR condition was as follows: 16°C for 30 min, 42°C for 30 min, 85°C for 5 min,
186 and 4°C until stopped. Real-time PCR was performed by using TaqMan-based PCR master
187 mix and detection primers miR-193a and U6snsubRNA (Thermo Fisher) in ABI-7500,
188 Applied Biosystems. For real-time PCR a 10 μl reaction mix was prepared containing
189 TaqMan PCR master mix II (5 μl), cDNA (2 μl), nuclease free water (2 μl), and primer (1 μl).
190 The qPCR conditions were as follows: 50°C for 2 min 95°C for 10 min, followed by 40
191 cycles of 95°C for 15 s, 60°C for 1 min. U6 was used as an internal control. Relative
192 quantification of gene expression was calculated using the $\Delta\Delta CT$ method and the results
193 were normalized to U6-snuRNA expression.

194 **Immunofluorescence detection of APOL1**

195 Control and experimental podocytes were fixed and permeabilized with a buffer containing
196 0.02% Triton X-100 and 4% formaldehyde in PBS. Fixed cells were washed three times in
197 PBS and blocked in 10% BSA for 60 min at 37°C. Subsequently, cells were labeled with
198 anti-APOL1 (Proteintech, IL). DAPI was used for nuclear localization. Control and
199 experimental cells were examined under immunofluorescence microscope.

200 **Western blotting studies**

201 Western blotting studies were carried out as described previously (4, 17, 22). Briefly,
202 control and experimental cells were harvested, lysed in RIPA buffer containing 50 mM Tris-
203 Cl (pH 7.5), 150 mM NaCl, 1mM EDTA, 1% NP-40, 0.25% Deoxycholate, 0.1% SDS, 1X
204 protease inhibitor cocktail (Calbiochem, Cocktail Set I), 1mM PMSF, and 0.2mM sodium
205 orthovanadate. Protein concentration was measured using Biorad Protein Assay kit. Total
206 protein lysed extracts (30 µg/lane) were loaded on a 10 % polyacrylamide (PAGE) premade
207 gel (Bio-Rad) and transferred onto PVDF membranes were processed for immunostaining
208 with primary antibodies against APOL1 (mouse monoclonal, 1:1000, Protein tech), WT1
209 (rabbit polyclonal, 1:1000, Abcam, MA), PAX2 (rabbit polyclonal, 1:800, Abcam), Menin
210 (mouse monoclonal, 1:1000, Santa Cruz), DNMT1 (mouse monoclonal, 1:1000, Santa
211 Cruz), EZH2 (Goat polyclonal, 1:1000, Santa Cruz), RBBP4 (Rabbit polyclonal, 1:1000,
212 Santa Cruz), and H3K27me3 (rabbit polyclonal, 1:1000, Cell Signaling Technologies, MA),
213 podocalyxin (rabbit polyclonal, 1:1000, Thermo Fisher) and nephrin (rabbit polyclonal,
214 1:800, Abcam) followed by treating with horseradish peroxidase labeled appropriate
215 secondary antibodies. The blots were developed using a chemiluminescence detection kit

216 (PIERCE, Rockford, IL) and exposed to X-ray film (Eastman Kodak Co., Rochester, NY).
217 Equal protein loading and the protein transfer were confirmed by immunoblotting for
218 determination of actin/GAPDH protein using a polyclonal β -Actin/GAPDH antibody (Santa
219 Cruz, CA) on the same (stripped) western blots.

220 **Immunoprecipitation (IP)**

221 Lysates from undifferentiated and differentiated PDs were first immunoprecipitated following
222 the addition of 5 μ g of monoclonal antibody to WT1 (Santa Cruz Biotechnology). The
223 immune complexes were then collected using 25 μ l of Protein-A + G sepharose beads (GE
224 Health Care, Life Science), in RIPA buffer. The IP was carried out at 4°C, for 4h, on a
225 rotating platform. Following this, precipitated A/G proteins were pelleted down by
226 centrifugation at 4,500 rpm for 10 min at 4°C. Next, the protein pellet was washed (3X)
227 each time with 1 ml of cold RIPA lysis buffer followed by centrifugation each time for 10
228 minutes at 2,500 rpm in a microfuge. After washings, beads were re-suspended in 100 μ l of
229 lysis buffer to which SDS-PAGE sample buffer (50 μ l) was added and samples were boiled
230 at 100°C, followed by SDS-PAGE and immunoblotted using specific antibodies as indicated.

231 **Statistical analyses**

232 Statistical comparisons were performed with the program PRISM using the Mann–
233 Whitney *U* test for nonparametric data and the unpaired *t* test for parametric data.
234 A *P* value < 0.05 was accepted as statistically significant.

235

236

237

238

239 **Results**

240 **High glucose causes dedifferentiation of podocytes**

241 Dedifferentiation of PDs is characterized by enhanced expression of PAX2 and down
242 regulation of WT1. To determine the effect of high glucose on PAX2 expression, Proteins
243 and RNAs were extracted from control and high glucose treated DPDs (n= 3). Protein blots
244 were probed for PAX2 and re-probed for actin. Gels from three different lysates are
245 displayed in Fig. 1A (Upper panel). Cumulative densitometric data are shown in bar graphs
246 (Lower panel, Fig. 1A). High glucose enhanced ($P<0.05$) expression of PAX2 in DPDs.
247 cDNAs were amplified with a specific primer for PAX2. Cumulative data on mRNA
248 expression of PAX2 are shown in Fig. 1C. High glucose also enhanced PAX2 mRNA
249 expression in DPDs. Protein blots of the same lysate preparations were probed for WT1
250 and re-probed for actin. Gels from three different lysates are displayed in Fig. 1 B (Upper
251 panel). Cumulative densitometric data are shown as a bar graph in the lower panel (Fig.
252 1B). cDNAs were amplified with a specific primer for WT1. Cumulative data are shown in a
253 bar graph (Fig.1 D). High glucose down regulated ($P<0.05$) WT1 mRNA as well as protein
254 expression in DPDs. These findings suggest that high glucose down regulates transcription
255 and translation of WT1 but enhances transcription of PAX2 in DPDs.

256 We examined whether there is a causal relationship between high glucose-induced
257 down regulation of WT1 and upregulation of PAX2 expression in DPDs. DPDs were
258 transfected with either scrambled (SCR) or WT1siRNA (n=3). Subsequently, protein blots
259 were probed for WT1 and re-probed for PAX2 and GAPDH. Gels from three different lysates
260 are displayed in Fig. 1E. Cumulative densitometric data are shown in Fig. 1F. DPDs

261 silenced for WT1 displayed enhanced ($P < 0.05$) PAX2 expression. These findings confirm
262 that down regulation of WT1 causes upregulation of PAX2 in DPDs.

263 **High glucose induces DPDs dedifferentiation through upregulation of miR193a**

264 Since miR193a is a negative regulator of WT1 in PDs (11), we asked whether high
265 glucose is down regulating WT1 via up regulation of miR193a. DPDs were incubated in
266 media containing either normal glucose (control, 5 mM) or high glucose (30 mM) for 48
267 hours ($n=3$). RNAs were extracted and assayed for miR193a. As shown in Fig. 2A, high
268 glucose enhanced expression of miR193a in DPDs.

269 To determine whether a specific miR193a inhibitor carries the potential to reverse
270 effect of high glucose milieu, DPDs were incubated in media containing normal glucose (5
271 mM, control), high glucose (30 mM), empty vector (pCMV-MIR 25 nM) with or without
272 miR193a inhibitor (25 nM, Applied Biosystems, Thermo Fisher) for 48 hours followed by
273 RNA extraction. RNAs were assayed for miR193a. High glucose enhanced ($P < 0.01$ the
274 expression of miR193a in DPDs; however this effect of high glucose was attenuated by
275 inhibition of miR193a (Fig. 2B).

276 We hypothesized that if high glucose induced dedifferentiation of DPDs through
277 upregulation of miR193a, then inhibition of miR193a in high glucose milieu would preserve
278 DPDs molecular phenotype. DPDs were incubated in media containing either normal
279 glucose (control, 5 mM), high glucose (30 mM), empty vector (pCMV-MIR, 25 nM) with or
280 without a specific inhibitor of miR193a (25 nM) for 48 hours ($n=3$). Proteins were extracted
281 and protein blots were probed for WT1 and reprobed for PAX2 and actin. Gels are
282 displayed in Fig. 2C. Cumulative densitometric data are shown as a bar diagram in Fig. 2D.

283 High glucose decreased ($P<0.05$) DPDs expression of WT1 and enhanced ($P<0.05$)
284 expression of PAX2. However, miR193a inhibitor prevented upregulation of PAX2 in high
285 glucose milieu. These findings confirm that high glucose induces dedifferentiation of DPDs
286 through upregulation of miR193a.

287 **High glucose down regulates DPDs expression of APOL1 through Upregulation of**
288 **miR193a**

289 To determine the dose-response effect of high glucose on APOL1 expression in
290 DPDs, cells were incubated in media containing variable concentrations of glucose (5, 10,
291 20, 30, 35 mM) for 48 hours ($n=3$). Protein blots were probed for APOL1 and reprobed for
292 GAPDH. Representative gels are displayed in Fig. 3A. Glucose down regulated APOL1
293 expression in DPDs at higher concentrations (30 mM and above).

294 To evaluate the APOL1s relationship with dedifferentiation markers, UNDPDs,
295 DPDs-treated with RPMI containing either conventional glucose (11 mM) or HG (30 mM)
296 for 48 hours were analyzed for dedifferentiation markers ($n=4$). Protein blots were probed
297 for APOL1 and reprobed for WT1, PAX2, and GAPDH. Gels of three different lysates are
298 displayed in Fig. 3B. Cumulative densitometric data are shown as a bar diagram (Fig. 3C).
299 DPDs displayed the expression of APOL1 and WT1 but attenuated expression of PAX2; on
300 the other hand, high glucose inhibited the expression of APOL1 and WT1 but enhanced the
301 expression PAX2. These findings suggest that down regulation of APOL1 in DPDs is
302 temporally associated with down regulation of WT1 and upregulation of PAX2 in high
303 glucose milieu.

304 To determine whether miR193a is regulating the expression of APOL1, DPDs were
305 incubated in media containing either normal glucose (5 mM), high glucose (30 mM), empty
306 vector (25 nM; pCMV-MIR) with or without miR193a inhibitor (25 nM) for 48 hours (n=3).
307 Proteins and RNAs were extracted. Protein blots were probed for APOL1 and reprobed for
308 GAPDH. Gels are displayed in the upper panel of Fig. 3D. Cumulative densitometric data
309 are shown in bar graphs (Fig. 3E). High glucose down regulated ($P<0.05$) APOL1
310 expression in DPDs; however, miR193a inhibitor enhanced ($P<0.05$) APOL1 expression in
311 high glucose milieu. RNAs were extracted from the lysates of 3D and cDNAs were
312 amplified with a specific primer for *APOL1*. Cumulative data are shown as a bar diagram
313 (Fig. 3F). High glucose down regulated *APOL1* mRNA expression; however, inhibition of
314 miR193a stimulated *APOL1* mRNA expression both in control and high glucose milieus.
315 These findings suggest that miR193a negatively regulates APOL1 expression in DPDs
316 under control as well as in high glucose milieus.

317 DPDs grown on coverslips were incubated in media containing either normal
318 glucose (C, 5 mM), high glucose (30 mM) with or without a miR193a inhibitor (miR, 25 nM)
319 for 48 hours (n=3) followed by immuno-labeling for APOL1. Subsequently, cells were
320 examined under a confocal microscope. Representative fluoromicrographs are shown in
321 Fig. 3G. High glucose down regulated APOL1 expression (green fluorescence) in DPDs,
322 however this effect of high glucose was mitigated by inhibition of miR193a.

323 To determine the effect of overexpression of miR193a on APOL1 expression, DPDs
324 were transfected with either empty vector (EV) or miR193a plasmid (n=3). Proteins and
325 RNAs were extracted. Protein blots were probed for WT1, PAX2, APOL1, and re-probed for
326 GAPDH. Gels from three different lysates are displayed in Fig. 4A. Cumulative

327 densitometric data are shown as a bar diagram in Fig. 4B. MiR193a-overexpressing DPDs
328 showed down regulation of *APOL1* and *WT1* but upregulation of *PAX2*. cDNAs were
329 amplified for *APOL1*. Cumulative data are shown in a bar diagram (Fig. 4C). DPDs
330 overexpressing miR193a showed down regulation of *APOL1* mRNA. These findings
331 confirm that miR193a negatively regulates expression of *APOL1* in DPDs.

332 **WT1 repressor complex preserves DPDs molecular phenotype**

333 To characterize the molecular phenotypes of undifferentiated (UND) and
334 differentiated PDs (DPD), protein blots of UNDPDs (0 day incubation) and DPDs (10 days
335 incubation) were probed for PDs (nephrin, and podocalyxin), PEC (*PAX2*) markers, *APOL1*,
336 components of WT1 repressor complex (*RBBP4*, *EZH2*, *Menin*, *H3K27me3*, and *DNMT1*),
337 and actin. Gels from three different lysates are displayed in Figs. 5A (PD and PEC
338 markers) and 5B (components of WT1 repressor complex, input for IP data). Cumulative
339 densitometric data from the lysates of Figs. 5A and 5B are shown as bar diagrams (Figs.
340 5C and 5D). DPDs (10 days incubation) displayed higher expression of *APOL1*, nephrin,
341 and podocalyxin (PDX) but lower expression of *PAX2* when compared to undifferentiated
342 PDs (0 day, Figs. 5A and 5C). Interestingly, DPDs (10 days incubation) displayed
343 enhanced expression of the components of WT1 repressor complex (Figs. 5B and 5D).

344 To confirm the composition of WT1 repressor complex, input lysates of UND and
345 DPD were immunoprecipitated (IP) with the anti-WT1 antibody. IP fractions were probed for
346 WT1, *RBBP4* (Polycomb group protein), *EZH2*, *Menin*, *H3K27me3*, *DNMT1*, and IgG. Gels
347 from three different IP fractions are displayed in Fig. 5E. Cumulative densitometric data
348 from the lysates are shown in bar graphs (Fig 5F). IP fractions of DPDs displayed
349 enhanced expression of WT1, *RBBP4*, *Menin*, *EZH2*, *H3K27me3*, and *DNMT1* when

350 compared to 0 day PDs. These findings confirm that WT1 repressor complex is composed
351 of WT1, RBBP4, Menin, EZH2, H3K27me3, and DNMT1.

352 We asked whether the integrity of WT1 repressor complex is critical for the
353 prevention of dedifferentiation of DPDs. DPDs were transfected with scrambled (SCR),
354 WT1 siRNA, DNMT1 siRNA or WT1 + DNMT1 siRNAs. After 48 hours, protein blots were
355 probed for PAX2, WT1, nephrin, podocalyxin (PDX), DNMT1, and reprobed for actin. Gels
356 from three different lysates are displayed in Fig. 5G. Cumulative densitometric data are
357 shown as a bar diagram in Fig. 5H. Lack of either WT1 or DNMT1 enhanced the
358 expression of PAX2. Interestingly, combined silencing of WT1 and DNMT1 displayed
359 additive effect on PAX2 expression. These findings suggest that disruption of WT1
360 repressor complexes de-represses the expression of PAX2.

361 **Role of APOL1 in preservation of DPDs molecular phenotype**

362 To determine the role of APOL1 in the preservation of the DPDs molecular
363 phenotype, DPDs were transfected with either control (scrambled, SCR) or APOL1 siRNA.
364 Proteins were extracted from control and transfected cells (n=3). Protein blots were probed
365 for APOL1 and reprobed for PAX2, WT1, and GAPDH. Gels from three different lysates are
366 displayed in Fig. 6A. Cumulative densitometric data are shown in a bar diagram (Fig. 6B).
367 APOL1 silenced DPDs displayed attenuated ($P<0.05$) expression of WT1 and enhanced
368 ($P<0.05$) expression of PAX2 when compared to control and SCR DPDs. These findings
369 indicate that APOL1 expression is critical for the preservation of DPDs molecular
370 phenotype.

371 To determine whether APOL1 would be preserving DPDs molecular phenotype
372 through alterations in miR193a expression, DPDs were transfected with either control
373 (scrambled, SCR) or APOL1 siRNA. RNAs were extracted from control and transfected
374 cells (n=3). RNAs were assayed for miR193a. Cumulative data are shown in a bar diagram
375 (Fig. 6C).

376 To establish a functional relationship between miR193a and APOL1, DPDs were
377 transfected with either control (scrambled, SCR) or APOL1 siRNA and incubated in media
378 with or without miR193a inhibitor (25 nM) for 48 hours (n=3). Protein blots were probed for
379 APOL1, WT1, PAX2 and GAPDH. Gels from three different lysates are displayed in Fig.
380 6D. Silencing of APOL1 in DPDs down regulated WT1 and enhanced the expression of
381 PAX2; however, inhibition of miR193a did not alter this effect of APOL1. These findings
382 suggest the importance of APOL1 expression to sustain the functionality of APOL1-
383 miR193a axis.

384 To determine whether, miR193a inhibitor is fully functional in APOL1-silenced PDs,
385 RNAs were extracted from the lysates of 6D. RNAs were assayed and cumulative data
386 (n=3) are shown in a bar diagram (Fig. 6E). miR193a inhibitor down regulated PDs
387 expression of miR193a in control conditions but could not do so in APOL1 silenced-PDs.
388 These findings suggest that APOL1 is required for the functionality of APOL1-miR193a axis
389 in DPDs.

390 **APOL1 negatively regulates miR193a expression in DPDs**

391 To confirm a relationship between APOL1 and miR193a, UNDPDs stably expressing vector
392 and overexpressing APOL1G0 were differentiated (incubation in RPMI containing 11 mM

393 glucose for 10 days). APOL1G0-expressing DPDs were transfected with either scrambled
394 or APOL1 siRNAs (n=6). After 48 hours, proteins and RNAs were extracted. Protein blots
395 were probed for APOL1 and reprobed for WT1, PAX2 and actin. Gels from three different
396 lysates are displayed in Fig. 7A. Cumulative densitometric data (n=6) are shown as a bar
397 diagram (Fig. 7B). DPDs overexpressing APOLG0 displayed enhanced expression of
398 APOL1 and WT1 but down regulation of PAX2; however, silencing of APOL1 reversed this
399 APOL1G0. RNAs were assayed for miR193a and cumulative data are shown as a bar
400 diagram (Fig. 7C). DPDs overexpressing APOLG0 displayed down regulation of miR93a
401 expression, however, silencing of APOL1 upregulated the expression of miR193a. These
402 findings confirm that APOL1 negatively controls the expression of miR193a.

403 **VDR agonist (VDA) preserves DPDs phenotype through modulation of miR193a-**
404 **APOL1 axis in high glucose milieu**

405 Vitamin D3 has been known to down regulate expression of miR193a in parietal
406 epithelial cells (20). To determine the effect of VDA on miR193a expression in UNDPDs,
407 UNDPDs were incubated in media containing either vehicle (0.1% DMSO) alone or
408 different concentrations of VDA (EB1089, 0, 1.0, 10.0, and 100.0 nM) for 48 hours (n=3).
409 RNAs were extracted and assayed for miR193a. Cumulative data are shown in a bar
410 diagram (Fig. 8A). VDA down regulated miR193a in UNDPDs in a dose-dependent manner.

411 To determine the effect of VDA on high glucose-induced modulation of miR193a,
412 DPDs were incubated in media containing either normal glucose (C, 5 mM), high glucose
413 (HG, 30 mM), vehicle (0.1% DMSO) with or without VDA (EB1089, 10 nM) for 48 hours
414 (n=3). RNAs were extracted and assayed for miR193a. Cumulative data are shown as a

415 bar diagram (Fig. 8B). High glucose enhanced ($P<0.01$) expression of miR193a in DPDs.
416 However, VDA inhibited high glucose-induced upregulation of DPDs expression of
417 miR193a.

418 To examine the effect of VDA on high glucose-induced down regulation of APOL1,
419 DPDs were incubated in media containing either normal glucose (C, 5mM), high glucose
420 (HG, 30 mM) with or without VDA (EB1089, 10 nM) for 48 hours ($n=3$). Protein blots were
421 probed for APOL1 and reprobed for GAPDH. Representative gels are displayed in Fig. 8C.
422 Cumulative densitometric data are shown in a bar diagram (Fig. 8D). High glucose down
423 regulated ($P<0.05$) APOL1 expression in DPDs; however, VDA enhanced APOL1
424 expression in high glucose milieu. These findings suggest that VDA has potential to
425 preserve DPDs expression of APOL1 in high glucose milieu.

426 To evaluate the effect of VDA on high glucose-induced dedifferentiation, DPDs were
427 incubated in media containing either normal glucose (C, 5mM), vehicle (Veh, 0.1% DMSO
428 high glucose (HG, 30 mM) with or without VDA (EB1089, 10 nM) for 48 hours ($n=3$). Protein
429 blots were probed for WT1, PAX2 and reprobed for GAPDH. Representative gels are
430 displayed in Fig. 8E. Cumulative densitometric data are shown in a bar diagram (Fig. 8F).
431 High glucose down regulated ($P<0.05$) DPDs expression of WT1 but enhanced ($P<0.05$)
432 the expression of PAX2. However, VDA enhanced the expression of WT1 under high
433 glucose milieu. Moreover, VDA down regulated high glucose-induced PAX2 expression in
434 DPDs. These findings suggest that VDA carries a potential to preserve DPDs molecular
435 profile in high glucose milieu.

436

437 **Discussion**

438 The present study demonstrated that high glucose (HG) induced dedifferentiation in
439 DPDs. High glucose enhanced PAX2 expression, a marker of podocyte dedifferentiation,
440 as a consequence of disruption of WT1 repressor complex. High glucose-induced DPDs
441 dedifferentiation was associated with a higher expression of miR193a and inhibition of
442 miR193a prevented DPDs dedifferentiation. DPDs overexpressing miR193a displayed
443 down regulation of APOL1 and enhanced expression of dedifferentiating markers;
444 conversely, silencing of miR193a enhanced the expression of APOL1 and also preserved
445 DPDs phenotype. Interestingly, high glucose also attenuated DPDs expression of APOL1.
446 Moreover, stably APOL1G0-overexpressing DPDs displayed the enhanced expression of
447 WT1 but attenuated expression of miR193a; nonetheless, silencing of APOL1 reversed
448 these effects. Since silencing of APOL1 enhanced miR193a expression as well as
449 dedifferentiation in DPDs, it appears that down regulation of APOL1 contributed to
450 enhanced miR193a expression in HG milieu. Vitamin D receptor agonist (VDA) down
451 regulated miR193a, upregulated APOL1 expression, and prevented dedifferentiation of
452 DPDs in HG milieu. These findings suggest a novel role of APOL1 in the preservation of
453 molecular phenotype of DPDs in high glucose milieu.

454 Expression of parietal epithelial proteins such as Claudin 1 and PAX2 in the
455 glomerular capillary tufts in diabetic nephropathy could be a consequence of the
456 replacement of PDs by PECs or PDs reversal to PECs phenotype. Chen et al
457 demonstrated that high glucose milieu enhanced PAX2 gene expression in mouse
458 embryonic mesenchymal epithelial cells and kidney explants (6). In an experimental model
459 of podocyte reporter mice, podocyte injury stimulated expression of PAX2 (34). Therefore,

460 expression of PAX2 by glomerular capillary epithelial cells may not be able to predict their
461 lineage.

462 WT1 has been reported to regulate PAX2 expression negatively through the
463 formation of a repressor complex (44). WT1 repressor complex containing PcG proteins,
464 EZH2, and Menin binds at PAX2 gene and has been demonstrated to decrease
465 transcription of PAX2 (40, 44). In the present study, high glucose down regulated WT1 and
466 decreased the transcription of PAX2 in DPDs. WT1 bound IP fraction revealed the
467 presence of PcG protein, EZH2, Menin and DNMT1. Silencing of WT1 or DNMT1 disrupted
468 the repressor complex and upregulated PAX2 expression in DPDs. These findings suggest
469 that high glucose-induced down regulation of WT1 and enhanced PAX2 expression
470 occurred through disruption of WT1 repressor complex. We have displayed proposed
471 composition of WT1 repressor complex on PAX2 in Fig. 9A. However, these observations
472 need to be confirmed *in vivo* studies.

473 MicroRNA193a has been demonstrated to regulate WT1 transcription inversely in
474 podocytes (14). miR193a transgenic mice displayed loss of WT1 by podocytes and
475 developed focal glomerular sclerosis (14). Notably, dedifferentiation of PDs in the form of
476 PAX2 expression was not studied in this model. In the present study, high glucose
477 enhanced expression of miR193a and down regulated WT1 expression in the podocytes.
478 Inhibition of miR193a caused upregulation of podocyte WT1 expression in high glucose
479 milieu, suggesting an inverse relationship between miR193a and WT1 in high glucose
480 milieu. Moreover, inhibition of miR193a upregulated PD expression of WT1 and down
481 regulated PAX2 expression in high glucose milieu. These findings suggest that modulation

482 of miR193a could be used as a therapeutic strategy to preserve podocyte molecular
483 integrity in high glucose milieu.

484 In the present study, high glucose-induced upregulation of miR193a displayed a
485 temporal relationship with down regulation of APOL1 expression in PDs. On the other
486 hand, APOL1-silenced PDs displayed upregulation of miR193a and over-expressing
487 APOL1-PDs showed down regulation of miR193a expression. These findings suggest a
488 negative feedback relationship between APOL1 and miR193a in PDs. As noted below, this
489 miR193a-mediated down regulation of APOL1 in high glucose milieu could provide an
490 explanation for the low or absence of any association of APOL1 renal risk variants with
491 diabetic kidney disease (13). On the other hand, down regulation of APOL1 was associated
492 with dedifferentiation of DPDs both in high glucose milieu as well as under control
493 conditions; while upregulation of APOL1 provided protection against dedifferentiation of
494 podocytes in high glucose milieu. Therefore, enhanced APOL1 expression could be
495 considered with caution as a strategy to preserve podocyte phenotype in high glucose or
496 related adverse milieus. However, in the absence of such adverse milieus it is considered
497 that APOL1 expression may be dispensable to kidney health (19).

498 Since LPS, TNF- α , HIV and IFN- γ have been reported to enhance expression of
499 APOL1 in podocytes (23, 24, 27), these agents could be used to prevent down regulation of
500 APOL1 in high glucose milieu. However, these agents are phlogogenic *de novo*, and would
501 not be suitable in chronic kidney disease-carrying pre-existing inflammatory milieu. In our
502 study, we observed that VDA not only down regulated miR193a but also enhanced PD
503 expression of APOL1 in high glucose milieu. Therefore, VDA could be used to provide
504 protection against dedifferentiation in high glucose milieu through enhanced PD expression

505 of APOL1. However, using VDA for increasing APOL1 in high glucose milieu would be
506 detrimental for PDs health if the host carries APOL1 risk alleles (3, 15, 23, 24). Therefore, it
507 would be mandatory to characterize the genetic profile of APOL1 before using VDA as a
508 therapeutic strategy to preserve PDs molecular phenotype in high glucose milieu.

509 Genetic epidemiology indicated that African Americans (AAs) carrying APOL1 risk
510 alleles (G1 and G2) are prone to develop chronic kidney diseases at higher rates with few
511 exceptions such as diabetic nephropathy when compared to European Americans (13, 21,
512 41). In the present study, high glucose milieu down regulated expression of APOL1 in
513 podocytes; therefore, high glucose milieu would also down regulate podocyte expression of
514 APOL1 risk alleles in Africans Americans carrying APOL1 risk alleles. Since enhanced
515 expression of APOL1 risk alleles has been reported to be cytotoxic to podocytes, down
516 regulation of APOL1 risk alleles in high glucose milieu is unlikely to modulate net outcome.
517 Therefore, our data are consistent with the epidemiologic observations (13).

518 We conclude that high glucose-induced up regulation of miR193a stimulated
519 attenuated expression of APOL1 manifesting in the form of DPDs dedifferentiation (Fig.
520 9B). This effect of high glucose could be prevented by VDA through the reversal of APOL1-
521 miR193 axis alterations.

522 **Acknowledgements**

523 This work was supported by grants RO1DK 098074, RO1DK084910, RO1 DK083931
524 (PCS) from National Institutes of Health, Bethesda, MD, Israel Science Foundation grant
525 890015, and support from the Ernest and Bonnie Beutler Fund of the Rambam Health Care
526 Campus.

527 **References**

- 528 1. Ambros V. microRNAs: tiny regulators with great potential. *Cell*. 107:823-6, 2001
- 529 2. Andeen NK, Nguyen TQ, Steegh F, Hudkins KL, Najafian B, Alpers CE. The
530 phenotypes of podocytes and parietal epithelial cells may overlap in diabetic
531 nephropathy. *Kidney Int*. 88:1099-107, 2015.
- 532 3. Beckerman P, Bi-Karchin J, Park AS, Qiu C, Dummer PD, Soomro I, Boustany-Kari
533 CM, Pullen SS, Miner JH, Hu CA, Rohacs T, Inoue K, Ishibe S, Saleem MA, Palmer
534 MB, Cuervo AM, Kopp JB, Susztak K. Transgenic expression of human APOL1 risk
535 variants in podocytes induces kidney disease in mice. *Nat Med*. 23: 429-438, 2017
- 536 4. Chandel N, Husain M, Goel H, Salhan D, Lan X, Malhotra A, McGowan J, Singhal
537 PC. VDR hypermethylation and HIV-induced T cell loss. *J Leukoc Biol*. 93:623-31,
538 2013.
- 539 5. Charest PM, Roth J. Localization of sialic acid in kidney glomeruli: regionalization in
540 the podocyte plasma membrane and loss in experimental nephrosis. *Proc Natl*
541 *AcadSci U S A*. 82:8508-12, 1985
- 542 6. Chen YW, Liu F, Tran S, Zhu Y, Hébert MJ, Ingelfinger JR, Zhang SL. Reactive
543 oxygen species and nuclear factor-kappa B pathway mediate high glucose-induced
544 Pax-2 gene expression in mouse embryonic mesenchymal epithelial cells and
545 kidney explants. *Kidney Int*. ;70:1607-15, 2006.
- 546 7. Dijkman HB, Weening JJ, Smeets B, Verrijp KC, van Kuppevelt TH, Assmann KK,
547 Steenbergen EJ, Wetzels JF. Proliferating cells in HIV and pamidronate-associated
548 collapsing focal segmental glomerulosclerosis are parietal epithelial cells. *Kidney Int*.
549 70:338-44, 2006.

- 550 8. Discenza MT, He S, Lee TH, Chu LL, Bolon B, Goodyer P, Eccles M, Pelletier
551 J.WT1 is a modifier of the Pax2 mutant phenotype: cooperation and interaction
552 between WT1 and Pax2. *Oncogene*. 22:8145-55, 2003
- 553 9. Dressler GR, Deutsch U, Chowdhury K, Nornes HO, Gruss P. Pax2, a new murine
554 paired-box-containing gene and its expression in the developing excretory system.
555 *Development*. 109:787-95, 1990.
- 556 10. Dressler GR, Woolf AS. Pax2 in development and renal disease. *Int J Dev Biol*.
557 43:463-8, 1999
- 558 11. Eccles MR, Wallis LJ, Fidler AE, Spurr NK, Goodfellow PJ, Reeve AE. Expression of
559 the PAX2 gene in human fetal kidney and Wilms' tumor. *Cell Growth Differ*. 3:279-
560 89, 1992
- 561 12. Fontaine F, Lecordier L, Vanwalleghem G, Uzureau P, Van Reet N, Fontaine M,
562 Tebabi P, Vanhollebeke B, Büscher P, Pérez-Morga D, Pays E. APOLs with low pH
563 dependence can kill all African trypanosomes. *Nat Microbiol*. 11:1500-1506, 2017
- 564 13. Friedman DJ, Kozlitina J, Genovese G, Jog P, Pollak MR: Population-based risk
565 assessment of APOL1 on renal disease. *J Am Soc Nephrol* 22: 2098–2105, 2011
- 566 14. Gebeshuber CA, Kornauth C, Dong L, Sierig R, Seibler J, Reiss M, Tauber S, Bilban
567 M, Wang S, Kain R, Böhmig GA, Moeller MJ, Gröne HJ, Englert C, Martinez J,
568 Kerjaschki D. Focal segmental glomerulosclerosis is induced by microRNA-193a and
569 its downregulation of WT1. *Nat Med*. 19:481-7, 2013.
- 570 15. Hayek SS, Koh KH, Grams ME, Wei C, Ko YA, Li J, Samelko B, Lee H, Dande RR,
571 Lee HW, Hahm E, Peev V, Tracy M, Tardi NJ, Gupta V, Altintas MM, Garborcauskas
572 G, Stojanovic N, Winkler CA, Lipkowitz MS, Tin A, Inker LA, Levey AS, Zeier M,

- 573 Freedman BI, Kopp JB, Skorecki K, Coresh J, Quyyumi AA, Sever S, Reiser J. A
574 tripartite complex of suPAR, APOL1 risk variants and α integrin on podocytes
575 mediates chronic kidney disease. *Nat Med.* 23:945-953, 2017.
- 576 16. Herman-Edelstein M, Thomas MC, Thallas-Bonke V, Saleem M, Cooper ME,
577 Kantharidis P. Dedifferentiation of immortalized human podocytes in response to
578 transforming growth factor- β : a model for diabetic podocytopathy. *Diabetes.*
579 60:1779-88, 2011
- 580 17. Husain M, Meggs LG, Vashistha H, Simoes S, Griffiths KO, Kumar D, Mikulak J,
581 Mathieson PW, Saleem MA, Del Valle L, Pina-Oviedo S, Wang JY, Seshan SV,
582 Malhotra A, Reiss K, Singhal PC. Inhibition of p66ShcA longevity gene rescues
583 podocytes from HIV-1-induced oxidative stress and apoptosis. *J Biol Chem.*
584 284:16648-58, 2009.
- 585 18. Imasawa T, Obre E, Bellance N, Lavie J, Imasawa T, Rigother C, Delmas Y, Combe
586 C, Lacombe D, Benard G, Claverol S, Bonneu M, Rossignol R. High
587 glucose reprograms human podocyte energy metabolism during differentiation and
588 diabetic nephropathy. *FASEB J.* 31:294-307, 2017.
- 589 19. Johnstone DB, Shegokar V, Nihalani D, et al. APOL1 null alleles from a rural village
590 in India do not correlate with glomerulosclerosis. *PLoS One.* 2012;7:e51546.
- 591 20. Kietzmann L, Guhr SS, Meyer TN, Ni L, Sachs M, Panzer U, Stahl RA, Saleem MA
592 Kerjaschki D, Gebeshuber CA, Meyer-Schwesinger C. MicroRNA-193a Regulates
593 the Transdifferentiation of Human Parietal Epithelial Cells toward a Podocyte
594 Phenotype. *J Am Soc Nephrol.* 26:1389-401, 2015.

- 595 21. Kopp JB, Nelson GW, Sampath K, Johnson RC, Genovese G, An P, Friedman D,
596 Briggs W, Dart R, Korbet S, Mokrzycki MH, Kimmel PL, Limou S, Ahuja TS, Berns
597 JS, Fryc J, Simon EE, Smith MC, Trachtman H, Michel DM, Schelling JR, Vlahov D,
598 Pollak M, Winkler CA : APOL1 genetic variants in focal segmental
599 glomerulosclerosis and HIV-associated nephropathy. *J Am Soc Nephrol* 22: 2129–
600 2137, 2011
- 601 22. Kumar D, Plagov A, Yadav I, Torri DD, Sayeneni S, Sagar A, Rai P, Adabala M,
602 Lederman R, Chandel N, Ding G, Malhotra A, Singhal PC. Inhibition of renin activity
603 slows down the progression of HIV-associated nephropathy. *Am J Physiol Renal*
604 *Physiol.* 303:F711-20, 2012.
- 605 23. Lan X, Jhaveri A, Cheng K, Wen H, Saleem MA, Mathieson PW, Mikulak J, Aviram
606 S, Malhotra A, Skorecki K, Singhal PC. APOL1 risk variants enhance podocyte
607 necrosis through compromising lysosomal membrane permeability. *Am J Physiol*
608 *Renal Physiol.* 307:F326-36, 2014.
- 609 24. Lan X, Wen H, Lederman R, Malhotra A, Mikulak J, Popik W, Skorecki K, Singhal
610 PC. Protein domains of APOL1 and its risk variants. *ExpMol Pathol.* 99:139-44, 2015
611 .PMID:26091559
- 612 25. Luna-Antonio BI, Rodriguez-Muñoz R, Namorado-Tonix C, Vergara P, Segovia J,
613 Reyes JL Gas1 expression in parietal cells of Bowman's capsule in experimental
614 diabetic nephropathy. *Histochem Cell Biol.* 148:33-47, 2017
- 615 26. Miesen L, Steenbergen E, Smeets B. Parietal cells-new perspectives in glomerular
616 disease. *Cell Tissue Res.* 369:237-244, 2017.

- 617 27. Mikulak J, Oriolo F, Portale F, Tentorio P, Lan X, Saleem MA, Skorecki K, Singhal
618 PC, Mavilio D. Impact of APOL1 polymorphism and IL-1 β priming in the entry and
619 persistence of HIV-1 in human podocytes. *Retrovirology*. 13:63, 2016.
- 620 28. Murer L, Caridi G, Della Vella M, Montini G, Carasi C, Ghiggeri G, Zacchello G.
621 Expression of nuclear transcription factor PAX2 in renal biopsies of juvenile
622 nephronophthisis. *Nephron*. 91:588-93, 2002.
- 623 29. Nassirpour R, Raj D, Townsend R, Argyropoulos C. MicroRNA biomarkers in clinical
624 renal disease: from diabetic nephropathy renal transplantation and beyond. *Food*
625 *Chem Toxicol*. 98:73-88, 2016.
- 626 30. Ohtaka A, Ootaka T, Sato H, Ito S. Phenotypic change of glomerular podocytes in
627 primary focal segmental glomerulosclerosis: developmental paradigm? *Nephrol Dial*
628 *Transplant*. 17 Suppl 9:11-5, 2002.
- 629 31. Ohtaka A, Ootaka T, Sato H, Soma J, Sato T, Saito T, Ito S. Significance of early
630 phenotypic change of glomerular podocytes detected by Pax2 in primary focal
631 segmental glomerulosclerosis. *Am J Kidney Dis*. 39:475-85, 2002.
- 632 32. Pavenstädt H, Kriz W, Kretzler M. Cell biology of the glomerular podocyte. *Physiol*
633 *Rev*. 83:253-307, 2003
- 634 33. Reiser J, Kriz W, Kretzler M, Munde IP. The glomerular slit diaphragm is a modified
635 adherens junction. *J Am Soc Nephrol*. 11:1-8, 2000
- 636 34. Ryan G, Steele-Perkins V, Morris JF, Rauscher FJ 3rd, Dressler GR. Repression of
637 Pax-2 by WT1 during normal kidney development. *Development*. 121:867-75, 1995
- 638 35. Miesen L, Steenbergen E, Smeets B. Parietal cells-new perspectives in glomerular
639 disease. *Cell Tissue Res*. 369:237-244, 2017.

- 640 36. Saleem MA, O'Hare MJ, Reiser J, Coward RJ, Inward CD, Farren T, Xing CY, Ni L,
641 Mathieson PW, Mundel P. conditionally immortalized human podocyte cell line
642 demonstrating nephrin and podocin expression. *J Am Soc Nephrol.* 13:630-8, 2002.
- 643 37. Stieger N, Worthmann K, Schiffer M. The role of metabolic and haemodynamic
644 factors in podocyte injury in diabetes. *Diabetes Metab Res Rev.* 27:207-15, 2011.
- 645 38. Suzuki T, Matsusaka T, Nakayama M, Asano T, Watanabe T, Ichikawa I, Nagata
646 M. Genetic podocyte lineage reveals progressive podocytopenia with parietal cell
647 hyperplasia in a murine model of cellular/collapsing focal segmental
648 glomerulosclerosis. *Am J Pathol.* 174(5):1675-82, 2009.
- 649 39. Torres M, Gómez-Pardo E, Dressler GR, Gruss P. Pax-2 controls multiple steps of
650 urogenital development. *Development.* 121:4057-65, 1995
- 651 40. Toska E, Roberts SG. Mechanisms of transcriptional regulation by WT1 (Wilms'
652 tumour 1). *Biochem J.* 461:15-32, 2014
- 653 41. Tzur S, Rosset S, Shemer R, Yudkovsky G, Selig S, Tarekegn A, Bekele E,
654 Bradman N, Wasser WG, Behar DM, Skorecki K. Missense mutations in the APOL1
655 gene are highly associated with end stage kidney disease risk previously attributed
656 to the MYH9 gene. *Hum Genet.* 128:345-50, 2010.
- 657 42. Vanhamme L, Paturiaux-Hanocq F, Poelvoorde P, Nolan DP, Lins L, Van Den
658 Abbeele J, Pays A, Tebabi P, Van Xong H, Jacquet A, Moguilevsky N, Dieu M, Kane
659 JP, De Baetselier P, Brasseur R, Pays E: Apolipoprotein L-I is the trypanosome lytic
660 factor of human serum. *Nature* 422: 83–87, 2003
- 661 43. Woolf AS, Winyard PJ. Gene expression and cell turnover in human renal dysplasia.
662 *Histol Histopathol.* 15:159-66, 2000.

663 44. Xu B, Zeng DQ, Wu Y, Zheng R, Gu L, Lin X, Hua X, Jin GH. Tumor suppressor
664 menin represses paired box gene 2 expression via Wilms tumor suppressor protein-
665 polycomb group complex. *J Biol Chem.* 286:13937-44, 2011

666

667

668

669

670

671

672

673

674

675

676

677

678

679

680

681

682

683

684

685

686

687 **Figure legends**

688 **Fig. 1.High glucose causes dedifferentiation of podocytes**

689 A. Differentiated podocytes (pre-incubated in RPMI 1640 media containing glucose [11
690 mM] at 37°C; DPDs) were incubated in media containing normal glucose (C, 5 mM)
691 or high glucose (HG, 30 mM) for 48 hours (n=3). Proteins were extracted. Protein
692 blots were probed for PAX2 and re-probed for actin. Gels from three different lysates
693 are displayed (Upper panel). Cumulative densitometric data are shown in bar graphs
694 (Lower panel). *P<0.05 compared with C.

695 B. Protein blots from the lysate preparations of 1A were probed for WT1 and re-probed
696 for actin. Gels from three different lysates are displayed. Cumulative data are shown
697 in a bar diagram. *P<0.05 compared with C.

698 C. RNAs were extracted from the lysates of 1A. cDNAs were amplified with a specific
699 primer for PAX2. Cumulative data on mRNA expression of PAX2 are shown.
700 *P<0.05 compared with C.

701 D. RNAs were extracted from the lysates of 1A. cDNAs were amplified with a specific
702 primer for WT1. Cumulative data on WT1 mRNA expression are shown. *P<0.05
703 compared with C.

704 E. DPDs were transfected with scrambled (SCR, 25 nM) or WT1 (25 nM) siRNAs with
705 Lipofectamine RNAiMAX transfection reagent according to manufacturer's protocol
706 and left in opti-MEMmedia for 48 hrs (n=3). Subsequently, proteins were extracted
707 and protein blots from control and transfected cells were probed for WT1 and
708 re-probed for PAX2 and GAPDH. Gels from three different lysates are displayed.

709 F. Cumulative densitometric data from the gels of 1E are shown in a bar diagram.

710 * <0.05 compared with respective C and SCR.

711 **Fig. 2.High glucose induces PDs dedifferentiation through upregulation of miR193a**

712 A. DPDs were incubated in media containing either normal glucose (control, 5 mM) or
713 high glucose (30 mM) for 48 hours (n=4). RNAs were extracted and assayed for
714 miR193a. Cumulative data are shown in a bar diagram. * $P<0.05$ compared with C.

715 B. DPDs were incubated in media containing either normal glucose (5 mM, control),
716 high glucose (30 mM), empty vector (25 nM; pCMV-MIR; using lipofectamine as a
717 carrier) with or without miR193a inhibitor (25 nM, plasmid-based inhibitor using
718 lipofectamine as a carrier) for 48 hours (n=3). RNAs were extracted and assayed
719 for miR193a. ** $P<0.01$ with other variables.

720 C. DPDs were incubated in media containing either normal glucose (control, 5 mM),
721 high glucose (30 mM) empty vector (25 nM) with/without a specific inhibitor of
722 miR193a (25 nM) (n=3). After 48 hours, proteins were extracted. Protein blots were
723 probed for WT1 and re-probed for PAX2 and actin. Gels are displayed.

724 D. Cumulative densitometric data from the protein blots of 2C. * $P<0.05$ compared to
725 other WT1/PAX2 variables; ^a $P<0.05$ compared to respective C.

726 **Fig. 3.High glucose Down regulates DPD expression of APOL1 through Upregulation**
727 **of miR193a**

728 A. DPDs were incubated in media containing different concentrations of glucose (5,
729 10, 20, 30, 35) for 48 hours (n=3). Protein blots were probed for APOL1 and re-
730 probed for GAPDH. Representative gels are displayed.

731 B. DPDs were incubated in media containing either conventional glucose (11 mM)
732 or HG (30 mm) for 48 hours. Proteins were extracted from UNDPDs and

733 experimental DPDs (n=4). Protein blots were probed for APOL1 and reprobed for
734 WT1, PAX2, and GAPDH. Gels of three different lysates are displayed.

735 C. Cumulative densitometric data of protein blots of 3B are shown in a bar diagram.
736 *P<0.05 compared to respective UNDPD and DPD/HG; **P<0.01 compared to
737 respective UNDPD and DPD/HG.

738 D. DPDs were incubated in media containing either normal glucose (5 mM), high
739 glucose (30 mM), empty vector (25 nM) with or without miR193a inhibitor (25 nm,
740 miR-Inh) for 48 hours (n=3). Proteins were extracted. Protein blots were probed
741 for APOL1 and re-probed for GAPDH. Gels are displayed.

742 E. Cumulative densitometric data are shown in bar graphs. *P<0.05 compared with C
743 and EV; ^aP<0.05 compared with HG alone.

744 F. RNAs were extracted from the lysate preparations of 3D and cDNAs were
745 amplified for *APOL1* mRNA. Cumulative data are shown in a bar diagram.
746 *P<0.05 compared with respective C and EV; **P<0.01 compared with C, EV,
747 and HG alone; ***P<0.001 compared with C, EV, and HG alone; ^aP<0.05
748 compared with miR-Inh alone.

749 G. DPDs grown on coverslips were incubated in media containing either normal
750 glucose (C), high glucose with or without a miR193a inhibitor (miR, 25 nM) for 48
751 hours (n=3) followed by immuno-labeling for APOL1. Subsequently, cells were
752 examined under a confocal microscope. Representative fluoromicrographs are
753 shown.

754 **Fig. 4. Overexpression of miR193a down regulates APOL1**

- 755 A. DPDs were transfected with either empty vector (EV) or miR193a plasmid (n=3).
756 Proteins were extracted. Protein blots were probed for WT1, PAX2, APOL1, and
757 re-probed for GAPDH. Gels from three different lysates are displayed.
- 758 B. Cumulative densitometric data from the lysates of 4A.*P<0.05 compared to
759 Control and EV; **P<0.01 compared to Control and EV.
- 760 C. RNAs were extracted from the lysates of 4A. cDNAs were amplified with a
761 specific primer for *APOL1*. *P<0.05 compared with other variables.

762 **Fig. 5. WT1 repressor complex preserves DPDs molecular phenotype**

- 763 A. Protein blots of UNDPDs (0 day incubation) and DPDs (10 day incubation) were
764 probed for PDs (nephrin, WT1, and podocalyxin) and PEC (PAX2) markers,
765 APOL1, and actin. Gels from three different lysates are displayed.
- 766 B. Protein blots from 5A were re-probed for the components of WT1 repressor
767 complex. Gels from three different lysates are displayed.
- 768 C. Cumulative densitometric data from the lysates of 5A are shown as a bar
769 diagram. *P<0.05 compared to respective 0 day.
- 770 D. Cumulative densitometric data from the lysates of 5B are shown as a bar
771 diagram. *P<0.05 compared to respective 0 day.
- 772 E. Lysates from 5A were immunoprecipitated (IP) with the anti-WT1 antibody. IP
773 fractions were probed for WT1, RBBP4 (Polycomb group protein), Menin,
774 H3K27me3, DNMT1, and IgG. Gels from three different IP fractions are
775 displayed.
- 776 F. Cumulative densitometric data from the lysates of 5E are shown as bar graphs.
777 *P<0.05 compared with respective 0 day.

778 **G.** DPDs were transfected with either scrambled (SCR), WT1 siRNA (25 nM),
779 DNMT1 (25 nM), WT1+DNMT1 siRNAs with Lipofectamine RNAiMAX
780 transfection reagent according to manufacturer's protocol and left in opti-
781 MEMmedia for 48 hrs (in WT1 + DNMT1 experiments, cells were exposed to WT1
782 siRNA for 48 hours and DNMT1 siRNA for 24 hours). Subsequently, proteins were
783 extracted. Protein blots were probed for PAX2, WT1, nephrin, podocalyxin
784 (PDX), DNMT1 and re-probed for actin. Gels from three different lysates are
785 displayed.

786 **H.** Cumulative densitometric data from the lysates of 5G are shown as a bar
787 diagram. *P<0.05 compared to C, SCR, and siRNADNMT1 in PAX2 variables;
788 **P<0.01 compared to C, SCR, and siRNADNMT1 in PAX2 variables; ^aP<0.05
789 compared with C and SCR in Nephrin variables; ^bP<0.05 compared with C and
790 SCR in PDX variables; ^cP<0.01 compared C and SCR in WT1 variables; ^dP<0.01
791 compared with siRNADNMT1, C and SCR in DNMT1 variables.

792 **Fig. 6.Role of APOL1 in preservation of DPDs molecular phenotype**

793 **A.** DPDs were transfected with either control (scrambled, SCR) or APOL1 siRNA.
794 Proteins were extracted from control and transfected cells (n=3).Protein blots were
795 probed for APOL1 and re-probed for PAX2, WT1, and GAPDH. Gels from three
796 different lysates are displayed.

797 **B.** Cumulative densitometric data of protein blots displayed in 6A. *P<0.05 compared
798 with respective APOL1, WT1, and PAX2 in control and SCR variables.

799 **C.** DPDs were transfected with either control (scrambled, SCR) or APOL1 siRNA.
800 RNAs were extracted from control and transfected cells (n=3) and assayed for

801 miR193a. Cumulative data are shown in a bar diagram. **P<0.01 compared with
802 other variables.

803 D. DPDs were transfected with either control (scrambled, SCR) or APOL1siRNA and
804 incubated in media with or without miR193a inhibitor for 48 hours (n=3). Protein blots
805 were probed for APOL1, WT1, PAX2 and GAPDH. Gels from three different lysates
806 are displayed.

807 E. RNAs were extracted from the lysate preparations of 6D and assayed for miR193a.
808 Cumulative data are shown in a bar diagram. *P<0.05 compared with control and
809 SCR; **P<0.01 compared with control, miR193a inh alone, and SCR; ^aP<0.05 with
810 all other variables.

811 **7. APOL1 negatively regulates miR193a expression in DPDs**

812 A. UNDPDs stably expressing vector and overexpressing APOL1G0 were incubated in
813 RPMI containing 11 mM glucose and 10% serum for 10 days at 37°C. APOL1G0-
814 expressing DPDs were transfected with either scrambled or APOL1 siRNAs (n=6).
815 After 48 hours, proteins were extracted from control (vector) and siRNA-transfected
816 cells. Protein blots were probed for APOL1 and reprobed for WT1, PAX2 and actin.
817 Representative gels from three different lysates are displayed.

818 B. Cumulative densitometric data (n=6) from the protein blots of 7A are shown in a bar
819 diagram. *P<0.05 compared with V and G0 APOL1 siRNA in WT1 and all other
820 variables in PAX2 proteins; **P<0.01 compared with V and G0 APOL1 siRNA in
821 APOL1 protein.

822 C. RNAs were extracted from the lysates of the protocol 7A. RNAs were assayed for
823 miR193a and cumulative data are shown in a bar diagram. *P<0.05 compared with
824 vector; **P<0.01 compared with vector; ***P<0.001 compared with G0 and G0/SCR.

825 **Fig. 8. VDR agonist (VDA) preserves DPDs phenotype through modulation of**
826 **miR193a-APOL1 axis in high glucose milieu**

827 A. UNDPDs were incubated in media containing either vehicle (0.1% DMSO) alone or
828 different concentrations of VDA (EB1089, 0, 1, 10, and 100 nM) for 48 hours (n=3).
829 RNAs were extracted and assayed for miR193a. Cumulative data are shown in a bar
830 diagram. *P<0.05 compared with vehicle (VDA, 0 nM), VDA, 0 and 1.0 nM; **P<0.01
831 compared with vehicle (VDA, 0 nM), VDA, 0 and 1.0 nM; ^aP<0.05 compared with
832 VDA, 10 nM.

833 B. DPDs were incubated in media containing normal glucose (C, 5mM), high glucose
834 (HG, 30 mM), vehicle (0.1% DMSO with or without VDA (EB1089, 10 nM) for 48
835 hours (n=3). RNAs were extracted and assayed for miR193a. Cumulative data are
836 shown in a bar diagram. **P<0.01 compared with other variables.

837 C. DPDs were incubated in media containing either normal glucose (C, 5mM), high
838 glucose (HG, 30 mM) with or without VDA (EB1089, 10 nM) for 48 hours (n=3).
839 Protein blots were probed for APOL1 and re-probed for GAPDH. Representative
840 gels are displayed.

841 D. Cumulative densitometric data from the lysates of 8C are shown in a bar diagram.
842 *<0.05 compared to C; ^aP<0.05 compared to HG alone.

843 E. DPDs were incubated in media containing either normal glucose (C, 5mM), vehicle
844 (Veh, 0.1% DMSO, high glucose (HG, 30 mM) with or without VDA (EB1089, 10 nM)

845 for 48 hours (n=3). Protein blots were probed for WT1, PAX2 and re-probed for
846 GAPDH. Representative gels are displayed.

847 F. Cumulative densitometric data from the protein blots of 8E are shown in a bar
848 diagram. *P<0.05 compared with respective all other variables.

849

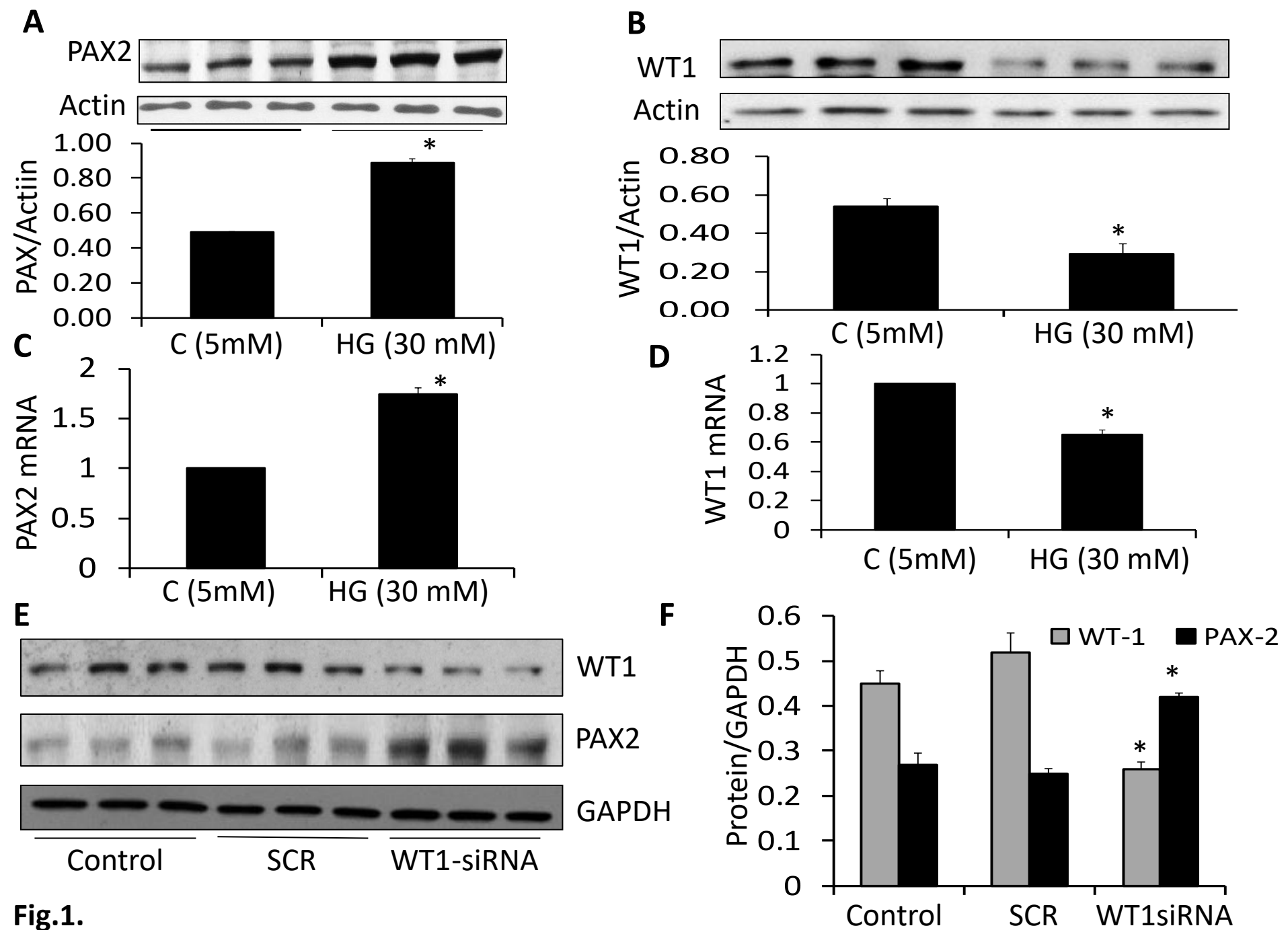
850 **Fig. 9. Proposed mechanistic schemes**

851 A. Composition of WT1 repressor complex is shown in a cartoon. WT1 repressor
852 complex binding to PAX2 promoter represses its transcription. Disruption of this
853 complex would de-repress the expression of PAX2.

854 B. High glucose enhanced the expression of miR193a, which led to down regulation of
855 APOL1 expression in DPDs. These alterations in miR193a-APOL1 axis induced
856 DPDs dedifferentiation. VDA provided protection against this effect of high glucose
857 through the reversal of miR193a-APOL1 axis alterations.

858

859



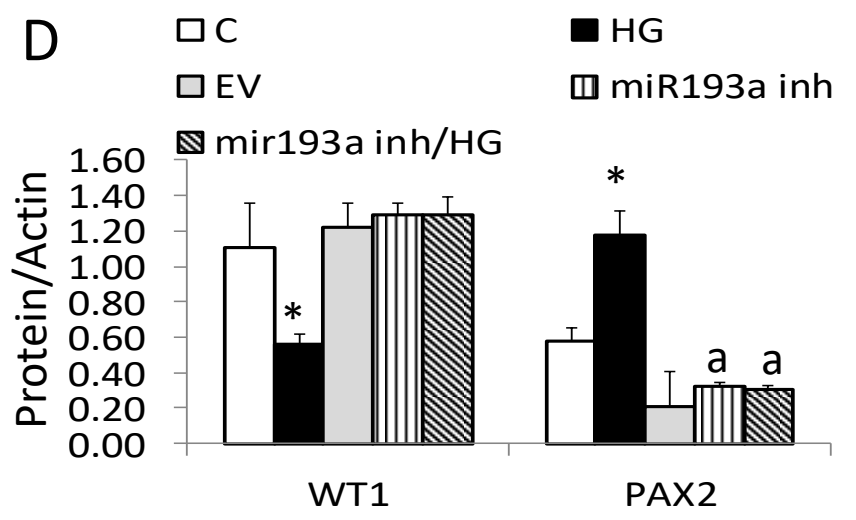
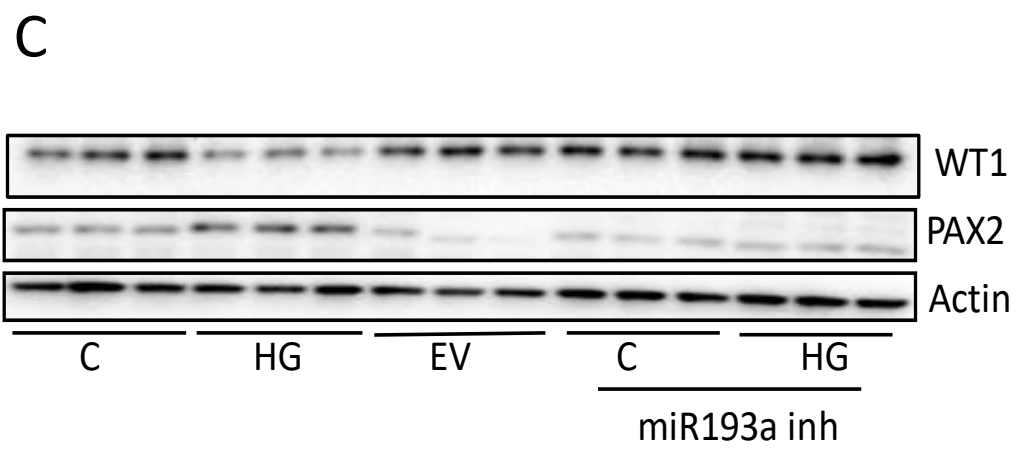
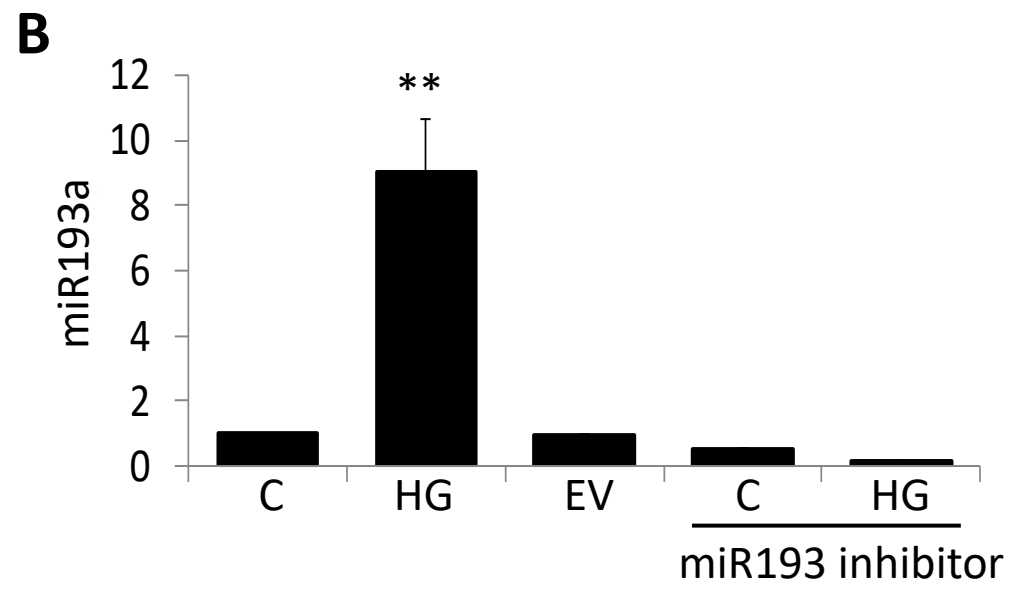
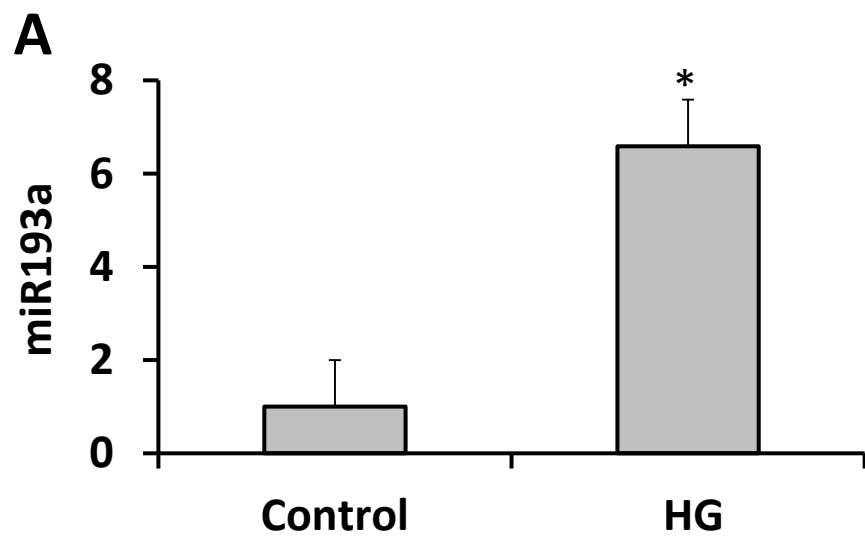


Fig. 2

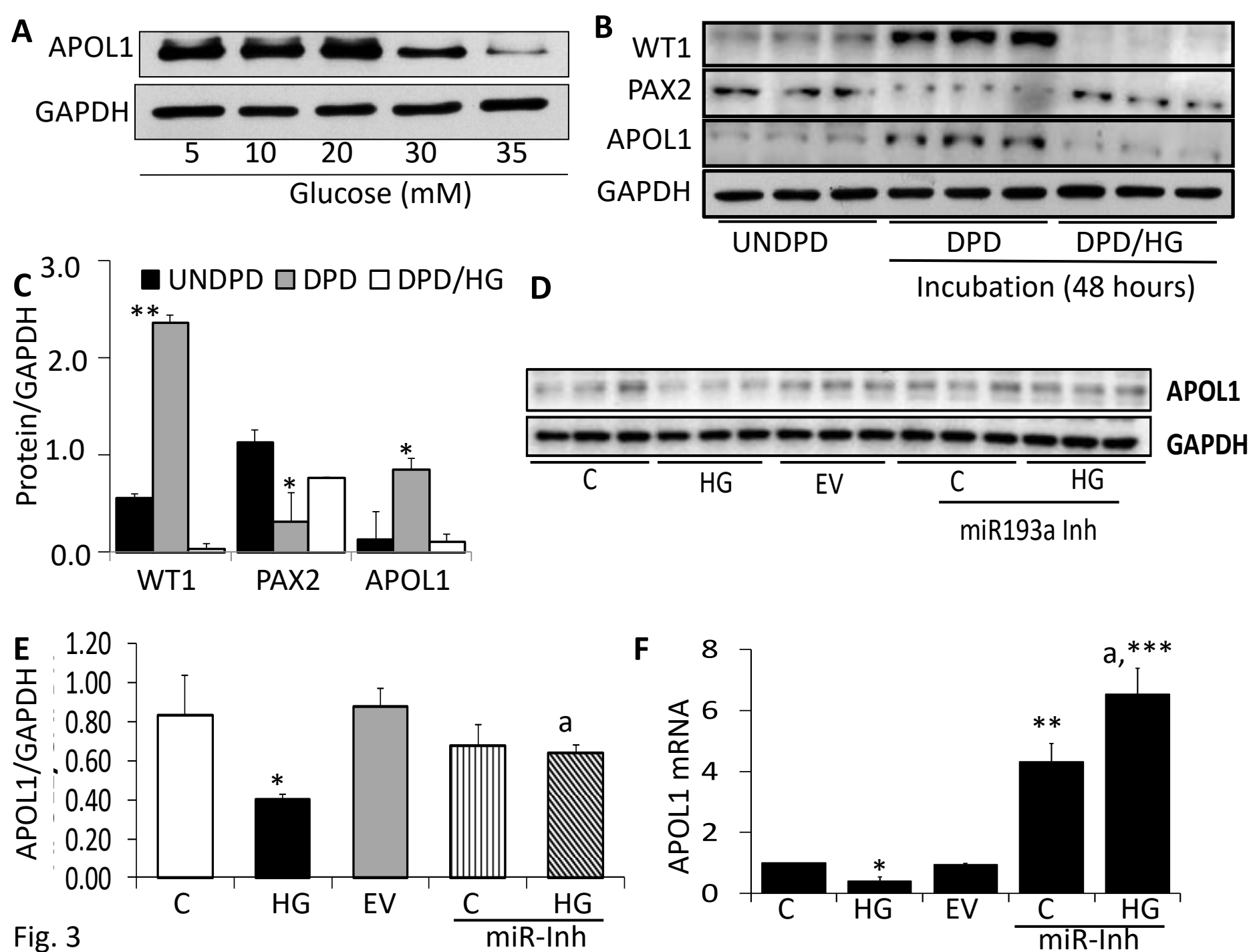


Fig. 3

G

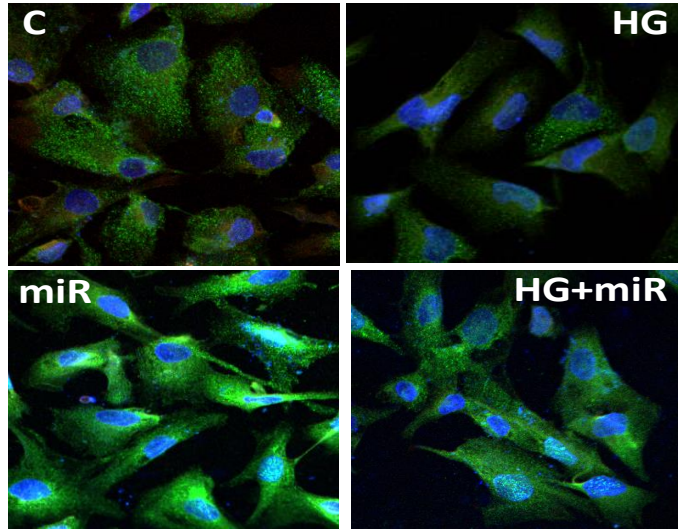
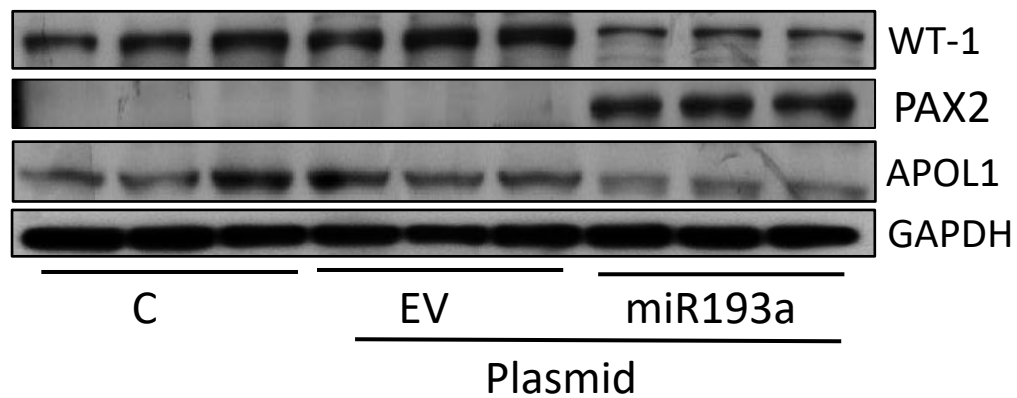
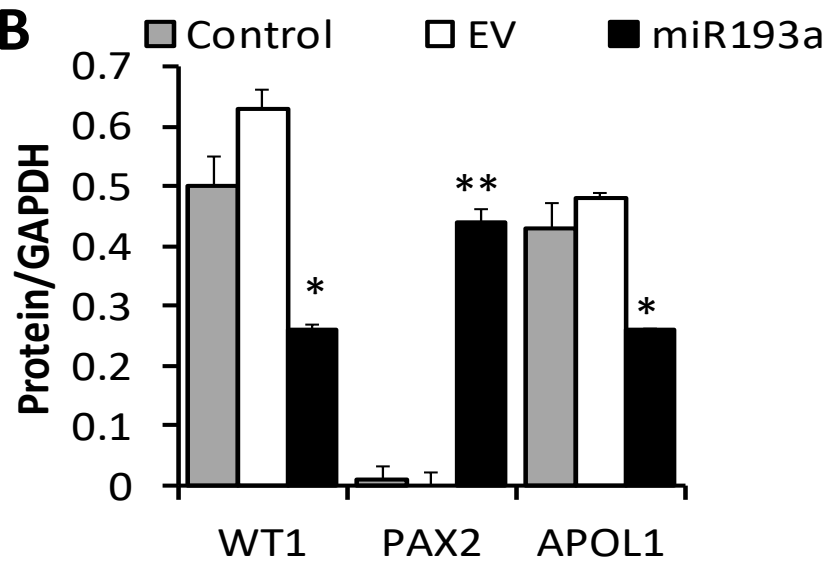
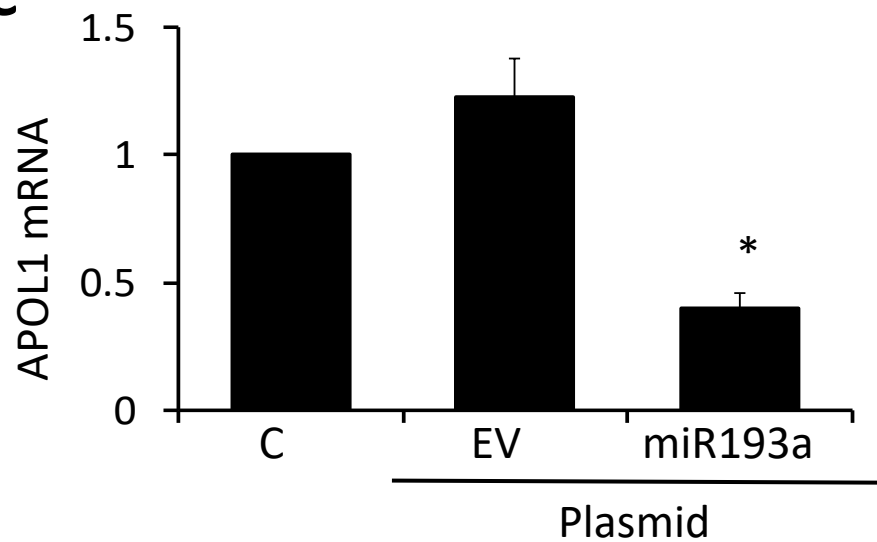


Fig. 3

A**B****C**

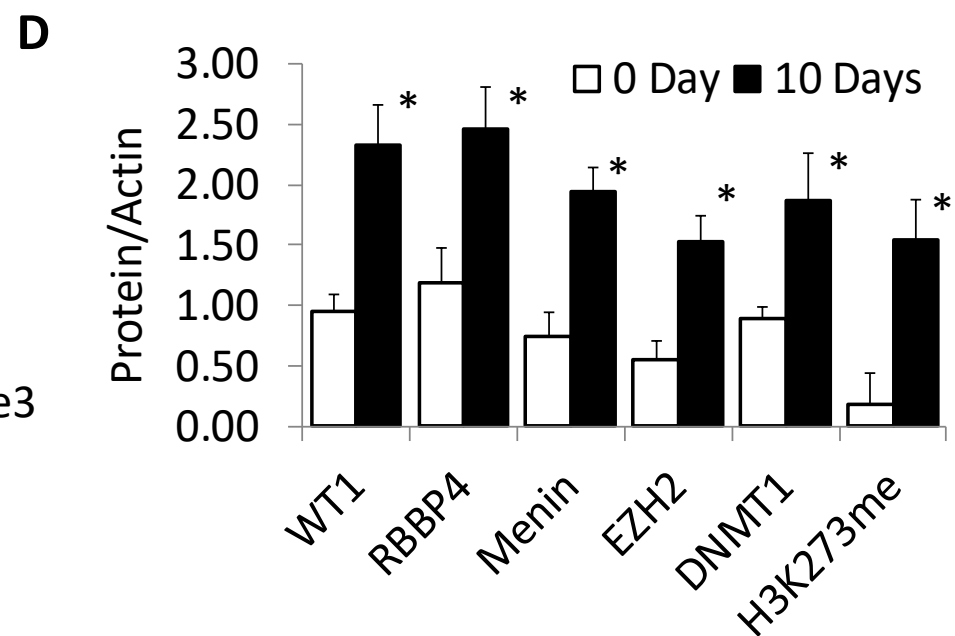
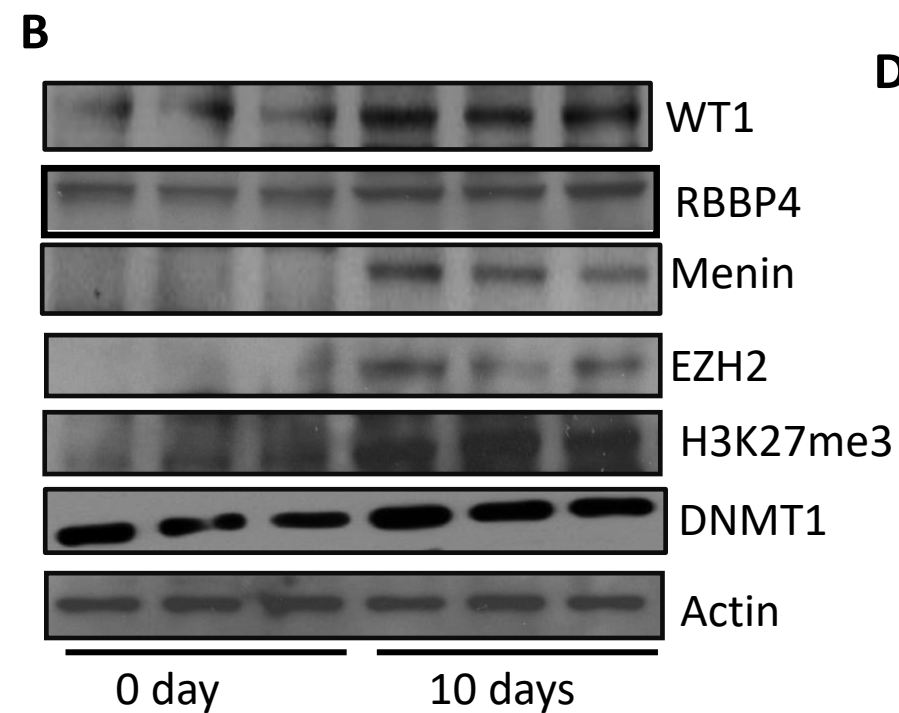
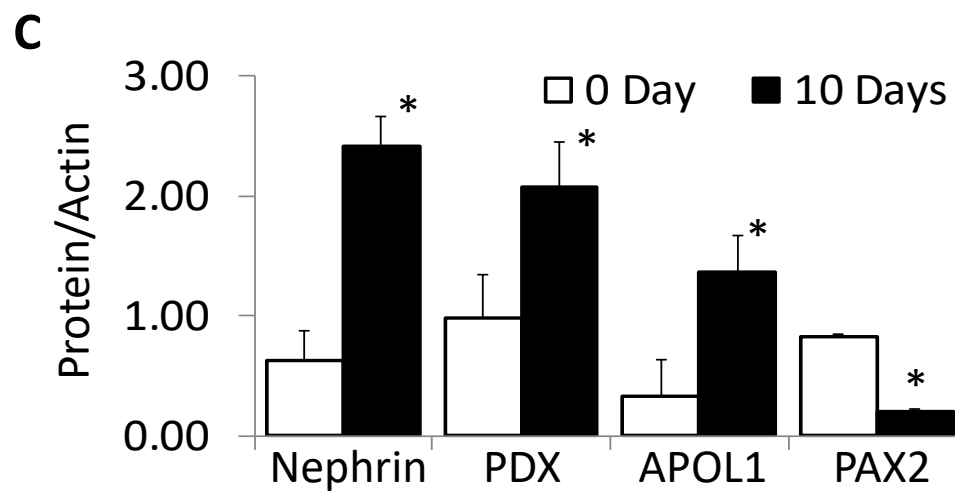
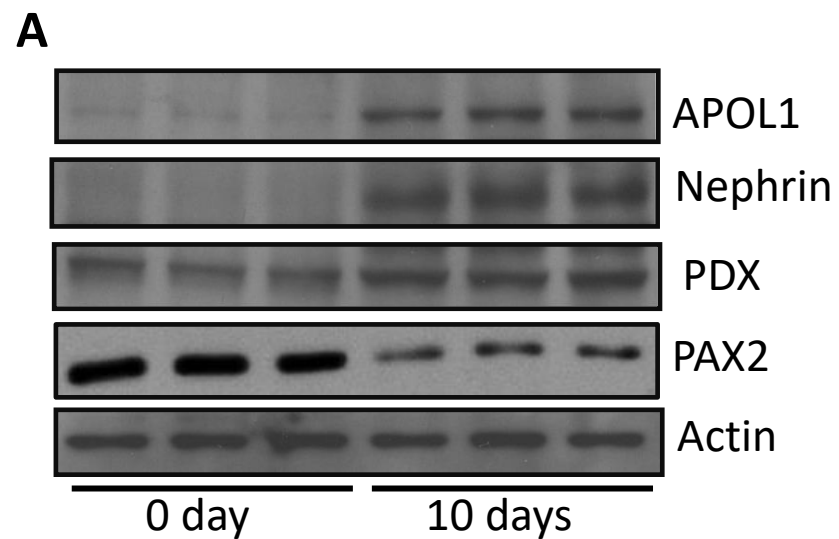


Fig. 5

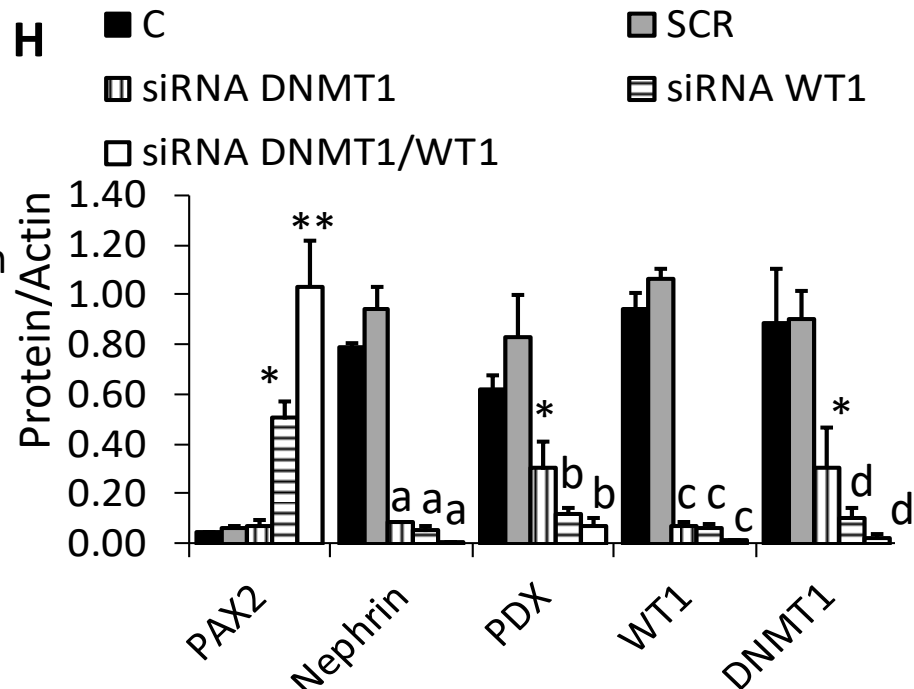
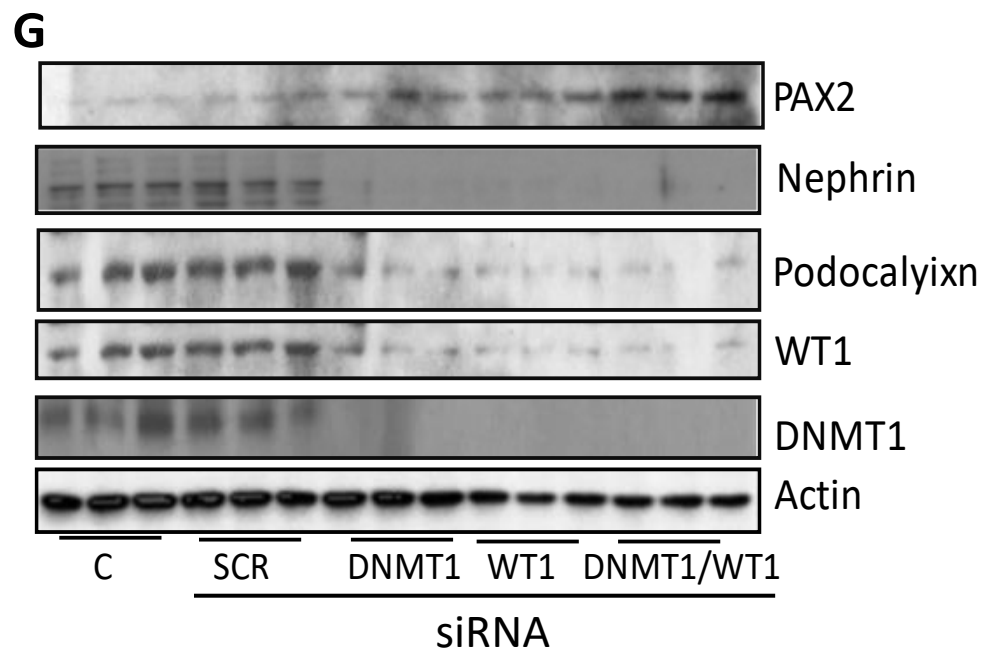
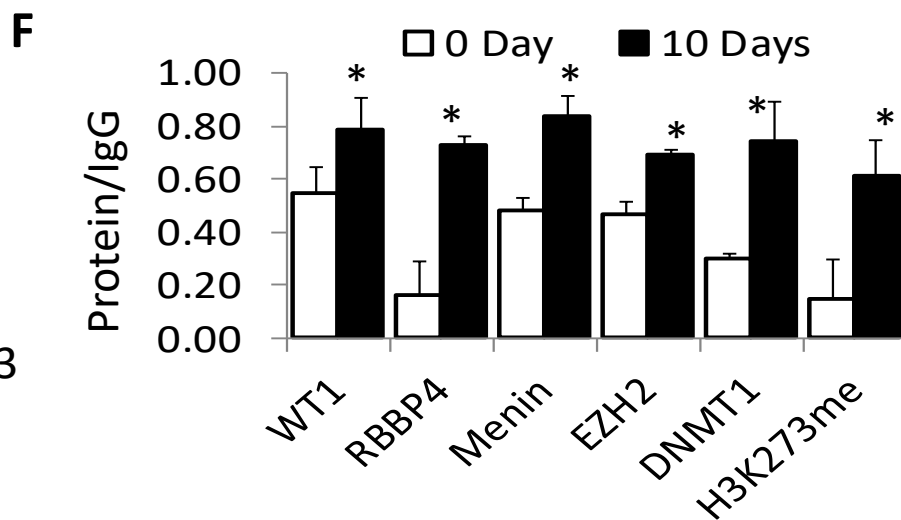
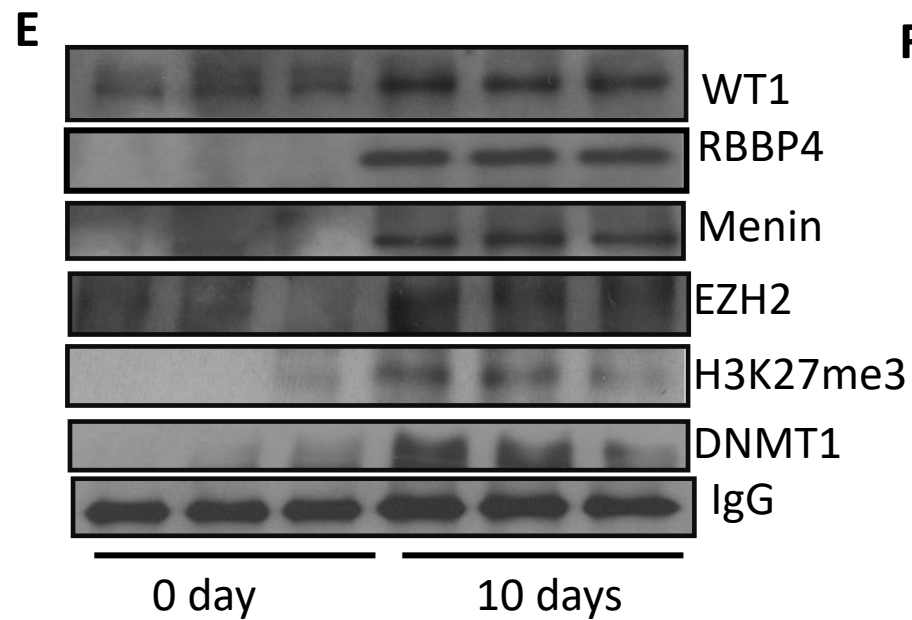


Fig. 5

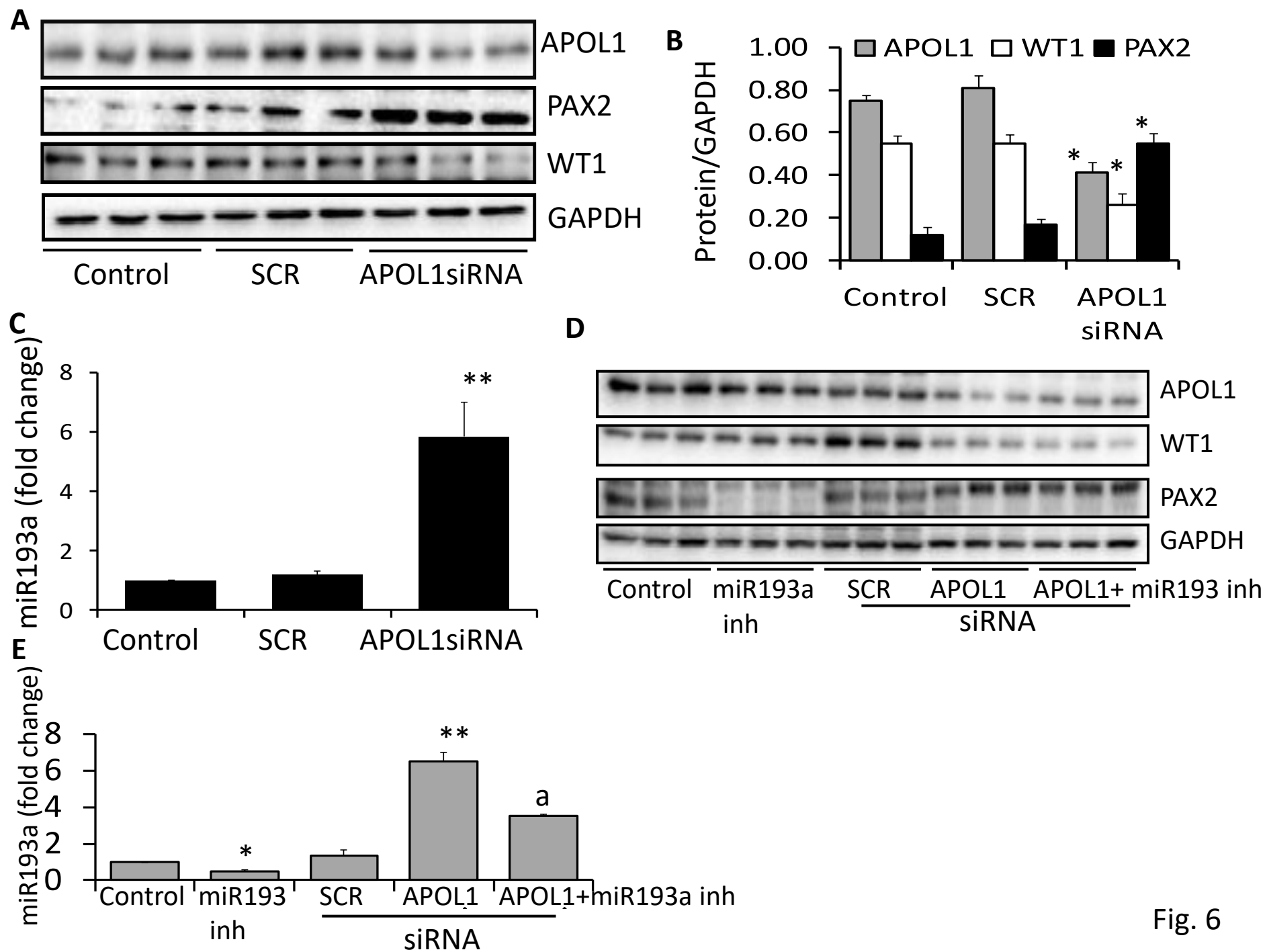


Fig. 6

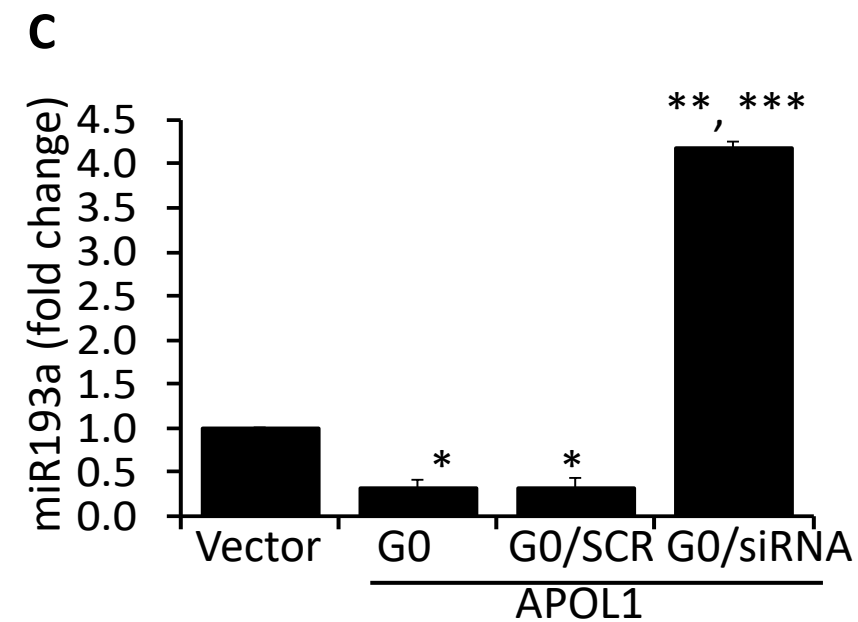
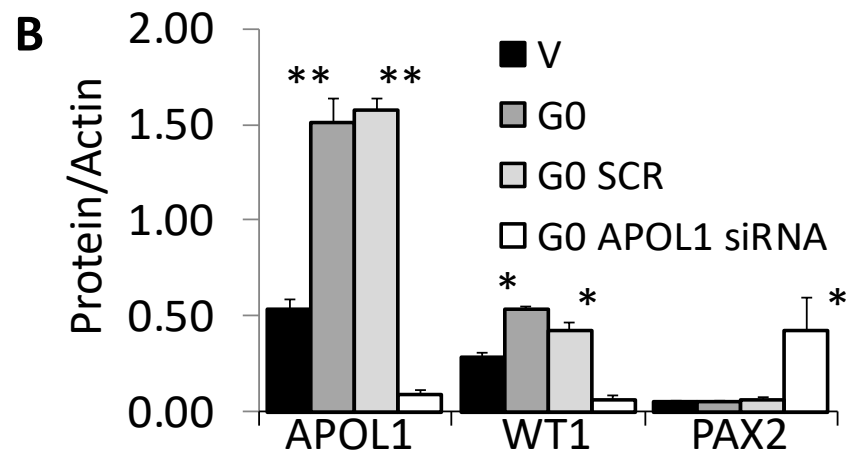
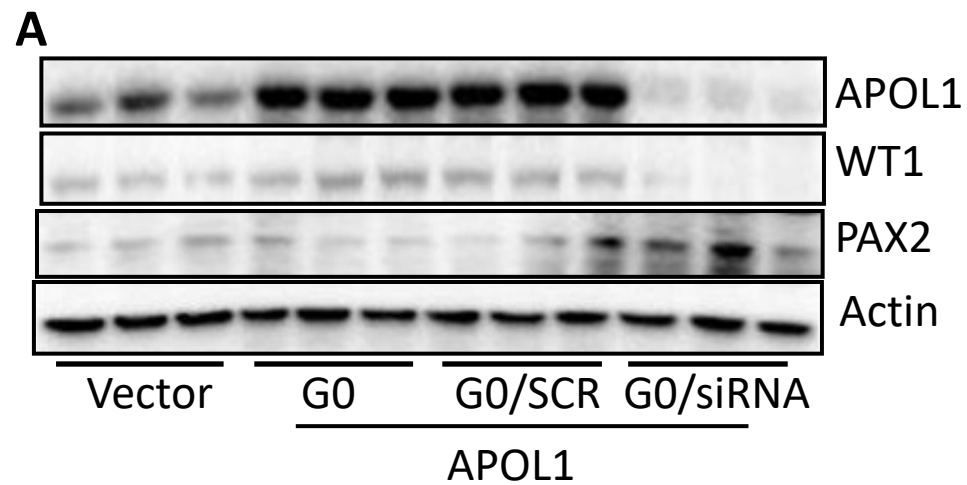


Fig. 7

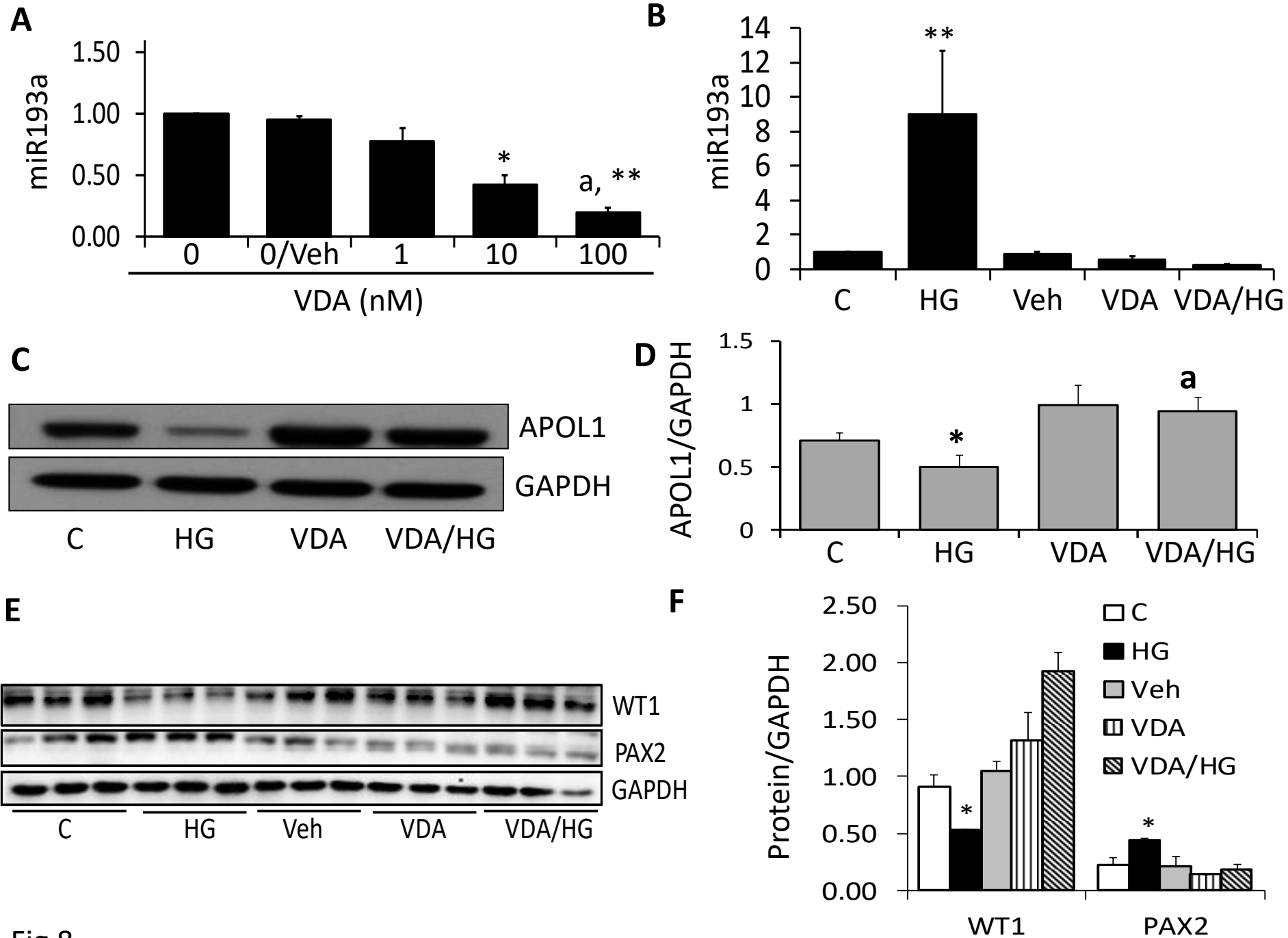


Fig.8

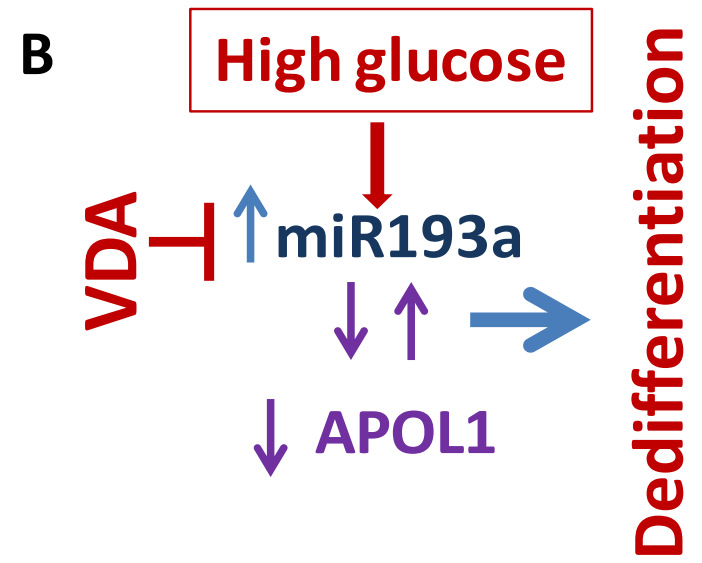
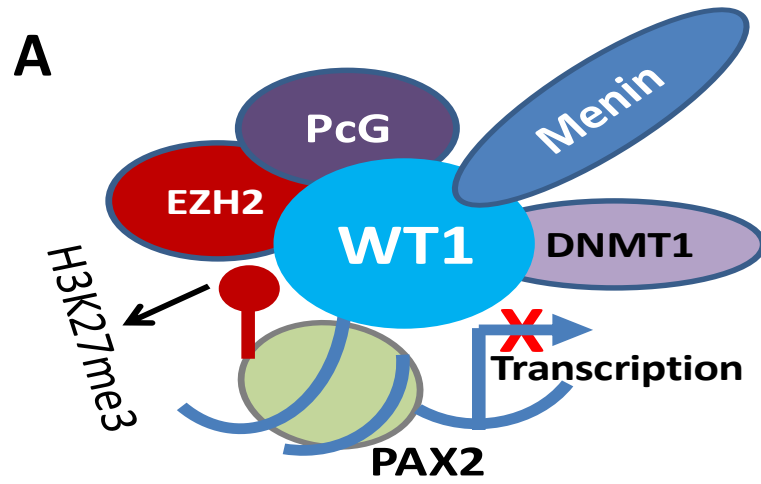


Fig. 9.